The Thesis committee for David E. Kaufman

Certifies that this is the approved version of the following thesis:

# Expanding the Applicability of Residential Economizers through HVAC Control Strategies

**Approved by**
**Supervising Committee:**

**Jeffrey A. Siegel, Supervisor**

**Atila Novoselac**

# Expanding the Applicability of Residential Economizers through HVAC Control Strategies

**by**

**David E. Kaufman, B.A.; M.S.; Ph.D.**

**Thesis**

Presented to the Faculty of the Graduate School of

The University of Texas at Austin

in Partial Fulfillment

of the Requirements

for the Degree of

**Master of Science in Engineering**

**The University of Texas at Austin**

**December 2009**

# Abstract

## Expanding the Applicability of Residential Economizers through HVAC Control Strategies

David E. Kaufman, M.S.E.

The University of Texas at Austin, 2009

Supervisor: Jeffrey A. Siegel

This study seeks to expand the range of climates and conditions in which free cooling from an economizer can replace air conditioning power consumption in residential applications. To explore this issue, we first discretize a simple building model in space and in time. We then solve the associated energy and mass balances for the estimated hourly heating and cooling loads and humidity conditions with respect to an annual climate profile.

We propose a forecast-based algorithm to control the rate of outdoor airflow brought in by an economizer, in response to the upcoming cooling load to be experienced by the interior airspace. The algorithm takes advantage of a range of acceptable temperatures for thermal comfort by precooling the envelope overnight to delay the onset of cooling demand during the day. In order to consider the highest potential benefit from

such an algorithm, we bypass the considerable problem of forecast accuracy by basing the inputs on the upcoming cooling load according to an initial simulation of the full year.

On the whole, even with the forecast-based control, the results of the study have much in common with previous findings in the literature. Precooling works better to reduce cooling load in cases of higher thermal and moisture mass, but a humid climate severely restricts when free cooling is beneficial. For the example house considered here with the Austin climate and other assumptions, the effect of the proposed forecast-based economizer control was to greatly reduce the indoor air cooling load while greatly increasing the number of annual hours of unacceptably high indoor humidity. When we adjusted the forecast-based algorithm to avoid the excess humidity, the remaining reduction in cooling load was not significant. To investigate further how a forecast-based economizer could reduce cooling load in humid climates, the prinicipal task should be to extend the control algorithm to forecast and manage upcoming indoor humidity levels in the same fashion as was done in this study for indoor air temperature.

# Table of Contents

# List of Tables

# List of Figures

# Chapter 1 Introduction and Literature Review

The objective of this study is to investigate the potential for a new approach to reduce residential air conditioning energy demands by cooling with outdoor air. Overall residential energy consumption takes up about 20% of national energy use (U.S. Department of Energy 2009), and Parker (2009) reports that alternative energy generation (e.g., photoelectric panels) must be balanced by energy efficiency improvements (e.g., passive solar design, advanced insulation) in order to achieve major residential energy savings in a cost-effective fashion. Cooling with outdoor air is one of the measures available for improving energy efficiency.

The topic of this thesis is to control the rate of airflow from outside according not only to current indoor and outdoor conditions but also with respect to conditions anticipated in the near future. The forecast-based element is intended to avoid overcooling the indoors beyond what would balance the upcoming heat transfer into the building, to prevent demands for otherwise unneeded heating that would be needed to maintain indoor thermal comfort conditions.

The building model and and analysis methodology will be highly simplified compared to a real case, but they will preserve important aspects of thermal and moisture mass that affect the evolution of indoor air conditions over time in response to HVAC and internal and external loads.

## 1.1 Economizers

Although natural ventilation by open windows is common in residential settings, the complex nature of air exchange rates under natural ventilation would be relatively difficult to address in an initial study. Therefore, we will take the simpler case of outdoor air exchange due to forced ventilation, i.e., fan-driven exchange via dedicated intake and exhaust outlets, at a variable airflow rate subject to control logic implemented by means of a duct damper and a variable-speed cycling fan motor. This HVAC capability is

commonly called an air-side economy cycle or *economizer* and is also described as *free cooling*, because it takes advantage of a temperature difference that is available without using air conditioning equipment.

There are two principal economizer modes: temperature-based and enthalpy-based (Spitler et al. 1987), also known as the dry-bulb economizer (DBE) and wet-bulb economizer (WBE) cycles. The temperature mode brings in outdoor air (above whatever minimum fresh air ventilation rate may be required for indoor air quality) when there is a cooling load on the indoor air and the ambient air is at a lower temperature. The enthalpy mode is similar, but by comparing enthalpy of indoor vs. outdoor air rather than temperature, it avoids bringing in outdoor air that is cooler but so humid that the additional latent cooling (dehumidification) load will outweigh the reduced sensible cooling load. Performing building energy simulations in various climates, Spitler et al. (1987) found that the performance improvements of the enthalpy mode over the temperature mode are very modest in principle and may be unattainable in practice due to the difficulty of reliable humidity measurement, except for the most humid climates. Their simulation examples showed energy savings ranging from 6% to 52% of cooling energy with DBE, and about 10% additional savings with WBE in very humid climates. Ke and Mumma (1999) showed that the energy efficiency contribution from economizer cycles also depends on air conditioning operating policies such as supply air temperature reset.

Recently, Lo (2005) studied an HVAC control algorithm for the Austin climate that included a DBE cycle modified to operate only when the outdoor relative humidity (RH) was below 80%. For the climate periods studied, the energy conservation benefits of the DBE were very small, because DBE operation was severely limited by the RH constraint and when operating, its benefits were often offset by electrical load for dehumidification.

## 1.2 Thermostatic Control Policies

The economizer models in the literature generally depend on a single thermostat setpoint temperature at any point in time. The setpoint may be different for heating vs. cooling and may vary with the building operating schedule, e.g., overnight setback allowing temperatures outside the thermal comfort range when the building is unoccupied. The control logic typically considers only the immediate moment, based on instantaneous weather conditions, heating/cooling load, and setpoint, without considering effects on succeeding periods.

Overnight setback works against the opportunity for free cooling. The higher overnight cooling setpoint calls for less overnight cooling just when cool outdoor air is most available. The air and thermal mass of the building are allowed to remain at or above the setpoint allowable for thermal comfort, hence in the daytime the HVAC system has to work against the heat being released by the building envelope to the indoor air (Braun et al. 2001). In commercial buildings, HVAC control for overnight thermal storage of cooling (i.e., load shifting by precooling) has been found to offer large cost savings up to 50% in simulations and experiments (Braun 1990; Morris et al. 1994). However, much of the savings comes from reduced peak load charges and load-shifting from on-peak to off-peak utility rates that are generally specific to commercial electricity billing, and from changes in air conditioner efficiency due to more balanced part-load conditions. This study instead focuses just on how economizer usage affects the cooling load on the airspace, taking into account forecast conditions in succeeding periods.

## 1.3 Building Modeling Approaches

One approach to studying the effects of forecast-based economizer controls would be to embed them in generally available building simulation software. Widely-used packages including DOE2 (Hirsch & Assoc. 2009), EnergyPlus (U.S. Department of Energy 2009), and TRNSYS (Thermal Energy System Specialists 2007) allow considerable customization of this kind, but at the cost of a very long learning curve.

Therefore, this study will proceed from a simple nodal (i.e., discretized in space) model of heat and moisture transfer and accumulation, modeled in systems of equations and solved for successive time periods. HVAC and economizer effects are incorporated directly into the equations and reflected in the resulting temperature and moisture profiles.

The test cases are drawn from the BESTEST methodology (Judkoff and Neymark 1995) that has been used to validate building energy simulation software, including DOE2, EnergyPlus, and TRNSYS, against measured energy consumption. The purpose of drawing on BESTEST is to ground the test cases in well-studied buildings. If we perform future studies using established building simulation software, the previously published results from BESTEST assessment of the software will be available as a baseline against which to evaluate the performance of new control algorithms.

## 1.4 Outline

Chapter 2 will describe the building to be studied and review the heat and mass transfer models to be solved for energy and moisture balance, including the effect of the HVAC system, in each hour of the simulated year.

Chapter 3 presents the full-year numerical solution method for the system without economizer and gives baseline results for energy consumption in the test cases.

Chapter 4 introduces economizer operation, in instantaneous and forecast-based modes, and shows how it affects the energy consumption and moisture profiles.

Chapter 5 reviews the results of the study and considers additional implications and directions for further study.

# Chapter 2 Building Model with Heat and Moisture Transfer

In keeping with the conceptual nature of the study, the building to be studied is a highly simplified residential building, essentially a closed box with a simple building envelope. The models for heat transfer and for moisture transfer have similar structure and will be solved separately in each time period. The models are linked, however, by the equilibrium temperature solution, which affects the vapor pressures in the moisture model through the ideal gas law. Thus the moisture model will be constructed numerically and solved based on the temperature solution of the heat transfer model for the same hour.

The mathematical model given here considers only one-dimensional heat transfer into and through the building envelope. It partitions the envelope layers that can absorb significant quantities of energy, to capture the delaying effect of such storage on the connection between outdoor conditions and indoor air conditions.

## 2.1 Building Characteristics

As mentioned in section 1.3, the structure of the building derives largely from the test cases in the BESTEST methodology for validation of building simulation software. The building is a simple rectangle, 6 m by 8 m with a height of 2.7 m. The walls consist of three layers, without considering any structural supports, thermal bridging, or corner effects. (The impact of these and other major assumptions are discussed in section 5.2.) There are two cases for the collection of building materials making up the walls, listing the materials in order from outside to inside: *lightweight* (wood siding; fiberglass quilt; plasterboard) and *heavyweight* (wood siding, foam insulation, and concrete block). The floor of the building consists of two layers: for the lightweight case, timber flooring resting on insulation, and for the heavyweight case, concrete slab resting on insulation. Table 2-1 lists the physical properties of materials for the two cases, including thickness $d$, density $\rho$, thermal conductivity $k$, and specific heat $c_P$, as specified by BESTEST.

The moisture-related properties (diffusivity and moisture content) will be discussed in section 2.4.

Table 2-1: Physical properties of lightweight building envelope

| Lightweight construction | | | | | | | |
|---|---|---|---|---|---|---|---|
| Material | Position | Conductivity $k$ (W/m·K) | Density $\rho$ (kg/m$^3$) | Specific heat $c_p$ (W/kg·K) | Thickness $d$ (m) | Diffusivity $D$ (kg/s·m·K) | Moisture capacity $\xi$ (scalar) |
| Wood siding | Wall, outer | 0.14 | 530 | 900 | 0.1 | $6.40 \cdot 10^{-13}$ | 0.20 |
| Fiberglass quilt | Wall, middle | 0.04 | 12 | 840 | 0.03 | $2.03 \cdot 10^{-10}$ | 0.06 |
| Plasterboard | Wall, inner | 0.16 | 950 | 840 | 0.01 | $2.72 \cdot 10^{-11}$ | 0.02 |
| Timber flooring | Floor, upper | 0.14 | 650 | 1200 | 0.025 | $6.40 \cdot 10^{-13}$ | 0.20 |
| Floor insulation | Floor, lower | 0.04 | 10 | 1400 | 1.003 | 0 | 0.02 |
| Heavyweight construction | | | | | | | |
| Material | Position | Conductivity $k$ (W/m·K) | Density $\rho$ (kg/m$^3$) | Specific heat $c_p$ (W/kg·K) | Thickness $d$ (m) | Diffusivity $D$ (kg/s·m·K) | Moisture capacity $\xi$ (scalar) |
| Wood siding | Wall, outer | 0.14 | 530 | 900 | 0.009 | $6.40 \cdot 10^{-13}$ | 0.00 |
| Foam insulation | Wall, middle | 0.04 | 10 | 1400 | 0.0615 | $2.50 \cdot 10^{-12}$ | 0.00 |
| Concrete block | Wall, inner | 0.51 | 1400 | 1000 | 0.1 | $2.74 \cdot 10^{-11}$ | 0.00 |
| Concrete slab | Floor, upper | 1.13 | 1400 | 1000 | 0.08 | $2.74 \cdot 10^{-11}$ | 0.00 |
| Floor insulation | Floor, lower | 0.04 | 10 | 1400 | 1.007 | 0 | 0.00 |

The building is assumed to have a fixed rate of infiltration of outdoor air into the interior, regardless of weather and wind conditions, of $\gamma_{inf} = 0.5$ air changes per hour (ACH). It is also assumed that the surface convection coefficients (to be applied in section 2.2.3) are fixed at specific values at all times: 8.29 W/m$^2$·K at indoor surfaces and 29.3 W/m$^2$·K at outdoor surfaces.

. This study further simplifies the building cases from BESTEST as follows:

- The four walls and the ceiling are represented together as a single one-dimensional layer, with a combined surface area and solar incident radiation.
- There are no windows or doors, so the envelope is opaque to solar radiation.
- There are no interior objects (e.g., furniture or carpeting) that can absorb energy or figure into heat transfer or accumulation.

These assumptions have varying degrees of impact. Assumptions such as single room, fixed convection coefficients, and no windows may be especially strong in

affecting the results to be obtained, but were important to make the analysis tractable. In comparison, the particular building materials and their properties may represent valid examples on a continuum of overall degrees of thermal and moisture mass. These impacts are discussed more fully in section 5.2.

## 2.2 Heat Transfer and Energy Balance

Each layer of the envelope, as well as the interior air space, must obey the law of conservation of energy, in that the energy it stores or releases at any point in time must be balanced by the net energy transferred into or out of it. Considering the layer as homogeneous and at a single temperature throughout, the energy balance takes the general form

$$\dot{E}_{st} = \dot{E}_{in} - \dot{E}_{out} + \dot{E}_g + \dot{E}_{sens} \tag{2.1}$$

This equation is developed in the rest of this section into the more detailed form

$$\rho V c_P \frac{dT}{dt} = \dot{E}_{conv} + \dot{E}_{cond} + \dot{E}_{rad} + \dot{E}_{inf} + \dot{E}_g + \dot{E}_{sens} \tag{2.2}$$

where

$\dot{E}_{st}$ = rate of thermal energy storage in material (W)

$\dot{E}_{in}$ = rate of heat flow into material (W)

$\dot{E}_{out}$ = rate of heat flow out of material (W)

$\dot{E}_g$ = rate of energy generation within material (W)

$\dot{E}_{sens}$ = rate of sensible heating or cooling delivered by HVAC system (W)

$\dot{E}_X$ = rate of energy input (W) due to specific heat transfer mechanism
$X \in$ {convection, conduction, radiation, infiltration}

$\rho$ = density (kg/m$^3$)

$V$ = volume (m$^3$)

$c_P$ = specific heat (J/kg·K)

$T$ = temperature (K)

$t$ = time (s)

The rest of this section reviews the mechanisms making up the terms of equation (2.1), potentially operating in parallel on a given building element. See Incropera et al. (2007), Chapters 3, 5, 6, and 13, for further details.

### 2.2.1 Energy Storage

For a building layer or airspace $i$, energy is accumulated proportionally to mass $m$ and specific heat $c_P$ as

$$\dot{E}_{st} = mc_P \frac{dT}{dt} = \rho V c_P \frac{dT}{dt} \tag{2.3}$$

In addition to the space discretization of building layers already discussed, we discretize the problem in time by estimating the temperature derivative as a finite difference between successive time intervals of duration $\Delta\tau$. If $\tau$ is the current time period and $\tau' = \tau - \Delta\tau$ is the preceding period, then

$$\dot{E}_{st} \approx \rho V c_P \frac{T(\tau) - T(\tau')}{\Delta\tau} \equiv \rho V c_P \frac{T - T'}{\Delta\tau} \tag{2.4}$$

### 2.2.2 Conduction

Under the one-dimensional steady-state version of Fourier's Law of Heat Conduction, the heat flux through a solid material layer with boundary temperatures $T_i$ and $T_j$ is proportional to the temperature difference:

$$\dot{E}_{cond} = \frac{kA}{d}(T_j - T_i) \tag{2.5}$$

for layers spaced at thickness $d$ with cross-sectional area $A$.

A layer may be external (solid layer on one side, air on the other), internal and homogenous (solid layers of the same material on either side), or internal and heterogeneous (solid layers of different materials on either side). For internal homogeneous layers, conduction occurs at both boundaries with the same physical properties but different temperature differences, e.g., $T_j - T_i$ and $T_k - T_i$. For internal heterogeneous layers, not only the temperature differences but also the physical properties are different on either side.

### 2.2.3 Convection

Under the steady-state version of Newton's Law of Cooling, the heat flow into a solid layer $i$ from an adjacent air space $j$ is

$$\dot{E}_{conv} = hA(T_j - T_i) \tag{2.6}$$

where the convection coefficient $h$ (W/m$^2$·K) depends on the geometry and orientation of the surface and on air velocity and other conditions. However, as noted in section 2.1, this study assumes fixed values $h$ as specified in the BESTEST cases.

### 2.2.4 Radiation

Surface $i$, not in contact with surface $j$ but with a sightline to it, exchanges energy by long-wave radiation approximately proportional to the difference in absolute temperatures to the fourth power, i.e.,

$$\dot{E}_{rad} = \sigma A_i \varepsilon_i \psi_{ij} (T_j^4 - T_i^4) \tag{2.7}$$

where $\psi_{ij}$ is a heat exchange factor related to the shape factor $F_{ij}$, which specifies the fraction of the radiation emitted by diffuse surface $i$ that would hit surface $j$ rather than any other surface in $i$'s line of sight.

For surfaces that are not part of an enclosure, such as radiation between an exterior wall and the ground, the heat exchange factor is $\psi_{ij} = \varepsilon_j F_{ij}$. For surfaces belonging to a closed envelope like the interior of the building, in general $\psi_{ij}$ is obtained by solving a linear system of equations. However, for the case of a two-surface enclosure (walls/ceiling and floor), a closed-form solution is available:

$$\psi_{ij} = \frac{\varepsilon_j F_{ij}}{(1-\varepsilon_i)\varepsilon_j F_{ij} + \varepsilon_i \varepsilon_j + (1-\varepsilon_j)\varepsilon_i F_{ji}} \tag{2.8}$$

Equation (2.7) can be written as

$$\dot{E}_{rad} = \sigma A_i \varepsilon_i \psi_{ij} (T_j - T_i)\left[h_r(T_i, T_j)\right] \tag{2.9}$$

where $h_r(T_i, T_j) = (T_i + T_j)(T_i^2 + T_j^2)$. In order to obtain a linear model, we will use equation (2.9) and approximate $h_r(T_i, T_j)$ by $h_r' \equiv h_r(T_i', T_j')$, using the temperatures

from the previous time period. The particular temperature variables on which $h_r'$ is based will be apparent from context.

For short-wave solar radiation, we bypass the geometric analysis needed to model insolation intensity, taking it instead as an output from the eQuest building energy simulation package as discussed in section 3.1. This is reduced by the external reflectivity to obtain the solar radiation absorbed by the building.

### 2.2.5 Infiltration

Energy is also transferred by the exchange of air mass between the indoor air space and the outdoor environment, often termed infiltration/exfiltration or building leakage. The difference in temperature between the entering air and the exiting air effects a net transfer of energy. The mass flow rate is determined from the infiltration air exchange rate $\gamma$ (air changes per hour, or ACH) and the volume $V_{air}$ of the indoor air space as

$$\dot{m}_{air} = \gamma \rho_{air} V_{air} \tag{2.10}$$

(neglecting variations in air density, which are relatively modest in the range of temperatures in question). Then the rate of heat transfer due to infiltration is proportional to the temperature difference between outdoor and indoor air:

$$\dot{E}_{inf} = \dot{m}_{air} c_{P,air} (T_{out} - T_{in}) \tag{2.11}$$

### 2.2.6 Energy Generation and HVAC

The term $\dot{E}_g$ in equation (2.1) represents heat released by conversion from other forms. In buildings, this is due mainly to electrical resistance heating from appliances, body heat from occupants, and combustion due to cooking. Per BESTEST, heat from internal generation will be assumed to be at a fixed rate $\dot{E}_g = 200\ W$, released directly to the indoor air by convection.

The term $\dot{E}_{sens}$ represents the sensible heating ($\dot{E}_{hvac} > 0$) or cooling ($\dot{E}_{hvac} < 0$) delivered by a central forced-air HVAC system to the interior space in response to

thermostatic control. Typically $\dot{E}_{sens} \neq 0$ only if room air would otherwise violate the allowable thermal comfort conditions. $\dot{E}_{sens}$ and $\dot{E}_g$ are added directly to the energy balance for the indoor air.

## 2.3 Building Discretization and System of Equations

A cross-section of the building envelope and interior is shown (not to scale) in Figure 2-1, with materials corresponding to the heavyweight case. In discretizing the envelope into layers, we divide the layers that have significant mass (wood siding and concrete) into two slices, to account for how their thermal mass delays the effect of ambient conditions on the interior. The wall insulation layer is thin and light, so its thermal mass is negligible and partitioning it is unnecessary. Recall that the four walls and the roof/ceiling are being simplified as a single one-dimensional layer (even though a concrete residential ceiling makes for an unlikely structural support requirement).

Node 1 therefore represents the outer quarter of the wood siding, node 2 the inner half, node 3 the inner quarter of wood siding and the outer half of the insulation layer, and so on. For simplicity, node 11 is assumed to remain at a fixed ground temperature of 10 °C, although this may lead us generally to underestimate heating and cooling loads for a slab-on-grade building. The same discretization structure is used for both building envelope cases.

### 2.3.1 Energy Balance Equation Structure

Since the energy balance equations are linear (by approximation) in the set of temperatures $\{T_1, T_2, \ldots, T_{11}\}$, the heat transfer interactions can be summarized in Table 2-2 as a linear system of 11 equations and 11 unknowns. Interactions are abbreviated as Ac = Accumulation, Cd = Conduction, Cv = Convection, R = Radiation, Inf = Infiltration, 1 = Constant. For example, a more complete form of the energy balance for node 1 is:

$$\rho_1 V_1 c_{P,1} \frac{T_1 - T_1{}'}{\Delta\tau} = \frac{k_1 A_1}{d_1}(T_2 - T_1) + h_1 A_1 (T_2 - T_1) + \sigma A_i \varepsilon_i \psi_{ij} h_r' (T_{sky} - T_1) + \sigma A_i \varepsilon_i \psi_{ij} h_r' (T_{grnd} - T_1) + \dot{E}_{solar} \quad (2.12)$$

from which linear terms of $T_1$ and $T_2$ can be collected on one side and constants (in this period) $T_1'$, $T_{sky}$, $T_{ground}$, and $\dot{E}_{solar}$ can be grouped on the other side.

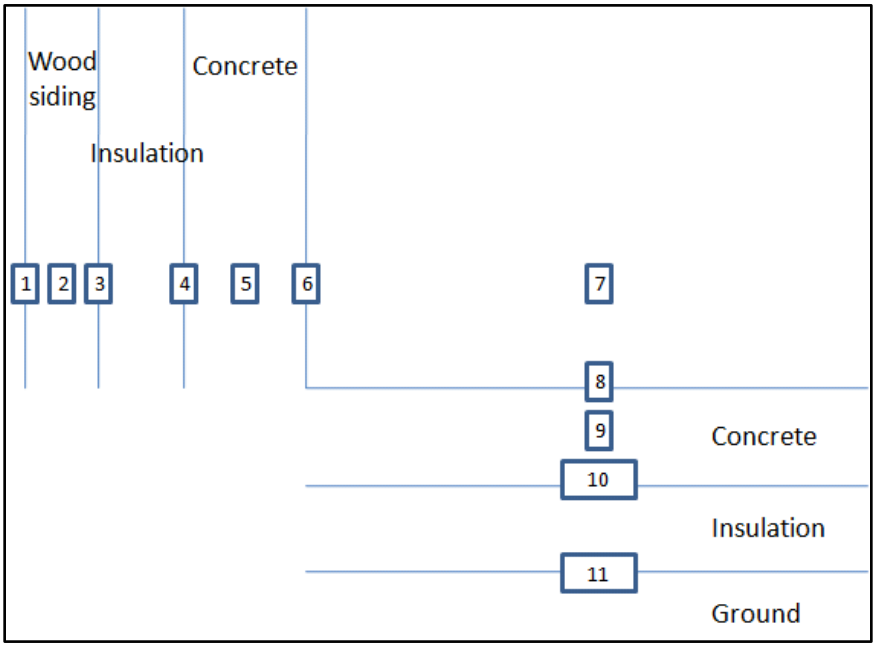


Figure 2-1: Discretization of building envelope (heavyweight)

Note the principal role to be played by the indoor air temperature $T_7$, as the main input to the building's thermostatic control and the main determinant of thermal comfort. Note also that this system of equations will be augmented in section 2.5 to be 12 x 12 rather than 11 x 11, to include the HVAC contribution $\dot{E}_{sens}$.

### 2.3.2 Uniform Temperature Assumption

In identifying a single temperature $T_j$ representing the state of any layer $j$ in a given hour, we are assuming a uniform temperature throughout the layer, under what is sometimes called the lumped capacitance model. For a solid material exchanging heat at its boundary by convection, this assumption is generally considered good if its Biot number satisfies $Bi = \frac{hd}{k} < 0.1$, and very poor if $Bi$ is greater than 1.

Table 2-2: System of energy balance equations

| | $T_1$ | $T_2$ | $T_3$ | $T_4$ | $T_5$ | $T_6$ | $T_7$ | $T_8$ | $T_9$ | $T_{10}$ | $T_{11}$ | $T'$ | $T_{amb}$ | $\dot{E}_{solar}$ | $T_{sky}$ | $T_{grnd}$ | $\dot{E}_g$ |
|---|---|---|---|---|---|---|---|---|---|---|---|---|---|---|---|---|---|
| 1 | Ac | Cd | | | | | | | | | | Ac | Cv | 1 | $R$ | $R$ | |
| 2 | Cd | Ac | Cd | | | | | | | | | Ac | | | | | |
| 3 | | Cd | Ac | Cd | | | | | | | | Ac | | | | | |
| 4 | | | Cd | Ac | Cd | | | | | | | Ac | | | | | |
| 5 | | | | Cd | Ac | Cd | | | | | | Ac | | | | | |
| 6 | | | | | Cd | Ac | Cv | R | | | | Ac | | | | | |
| 7 | | | | | | Cv | Ac | Cv | | | | Ac | Inf | | | | 1 |
| 8 | | | | | | R | Cv | Ac | Cd | | | Ac | | | | | |
| 9 | | | | | | | | Cd | Ac | Cd | | Ac | | | | | |
| 10 | | | | | | | | | Cd | Ac | Cd | Ac | | | | | |
| 11 | | | | | | | | | | | Ac | Ac | | | | | |

At the boundary of the wall, layers 1 and 6, we find $(Bi_1, Bi_6) = (0.47, 0.16)$ for the lightweight house and $(0.47, 0.41)$ for the heavyweight house. This indicates that the lumped assumption is less well-justified than is usually recommended. However, the building layers here are insulated not only by air layers but by relatively non-conductive solid layers, which should make the evenness of temperature within any one layer better than the standard Biot number would suggest. Compared to the degree of approximation being permitted in other parts of the model, the uniform temperature assumption seems acceptable here, so it is not necessary to improve it by more thinly discretizing the building material layers.

## 2.4 Mass Transfer and Moisture Balance

Just as energy is transferred with temperature difference as the driving force, moisture in the form of water vapor is transferred with partial pressure difference as the driving force. The transfer mechanisms are diffusion of mass through solid materials, in place of heat conduction, and convection mass transfer between solid and air space in place of heat convection. Moisture transport has no analogue to radiative heat transfer, and we neglect other mechanisms of moisture generation including internal loads due to occupants and condensation/evaporation. This section reviews the moisture transport mechanisms and equations, based on standard material covered in Incropera et al. (2007), Chapters 6 and 14 and ASHRAE (2005), Chapter 5.

### 2.4.1 Storage of Moisture Mass

For a building layer or airspace $i$, the stored mass of water vapor is $m_{st,i} = \rho_i V_i w_{st,i}$, where $w_{st,i}$ is the moisture content of element $i$, defined as kg of water vapor per kg of material. $w_{st,i}$ here plays a role analogous to $c_P$ in energy accumulation, and in solid materials even at equilibrium it varies widely according to the material and conditions including temperature and relative humidity. For example, Rode and Grau (2008) show a sorption curve for concrete, i.e., moisture content as a function of relative humidity $\varphi$, where the slope of the curve, also called the moisture capacity $\xi$, varies considerably with $\varphi$. However, we will simplify this by assuming a constant moisture capacity $\xi_i$ for material $i$, i.e., $w_{st,i} = \xi_i \varphi_i$ as listed in Table 2-1, based on representative values from sorption curves in Tye (1994), Table 6. If total moisture content affects indoor relative humidity more than incremental changes in moisture content, then the impact of this approximation is relatively mild.

Relative humidity relates to current vapor pressure and saturation vapor pressure $P_{sat}(T_i)$ (temperature-dependent) as $\varphi_i = P_i / P_{sat}(T_i)$. Thus for solid materials, approximating the pressure derivative by a finite difference as was done for temperature and considering $T_i$ to be fixed at its equilibrium value from the energy balance equations.

$$\dot{m}_{st} = \rho_i V_i \frac{dw_{st,i}}{dt} = \rho_i V_i \xi_i \frac{d\varphi_i}{dt} = \frac{\rho_i V_i \xi_i}{P_{sat}(T_i)} \frac{dP_i}{dt} \approx \frac{\rho_i V_i \xi_i}{P_{sat}(T_i)} \frac{P_i - P_i'}{\Delta\tau} \tag{2.13}$$

For airspace node 7, moisture accumulation can be addressed more simply in terms of the densities of water vapor $\rho_v$ and air $\rho_7$ within the air space:

$$w_{st,i} = \frac{\rho_v}{\rho_7} = \frac{P_i}{\rho_7 R_w T_7} \tag{2.14}$$

where $R_w = 461.5$ J/kg·K is the gas constant for water. This expression assumes the ideal gas law, which is usually considered a good assumption for air at ordinary temperatures and pressures.

The rate of moisture accumulation in moist air is then

$$\dot{m}_{st} = \rho_7 V_7 \frac{dw_{st}}{dt} = \frac{V_7}{R_w T_7} \frac{dP_7}{dt} \approx \frac{V_7}{R_w T_7} \frac{P_7 - P_7'}{\Delta\tau} \tag{2.15}$$

### 2.4.2 Diffusion

Under the one-dimensional steady-state version of Fick's Law of Diffusion, the heat flow through a solid material layer with boundary vapor pressures $P_i$ and $P_j$ is proportional to the pressure difference across the layer:

$$\dot{m}_{diff} = \frac{D_i A}{d} (P_j - P_i) \tag{2.16}$$

where $D_i$ is the diffusivity of moisture in the material. The diffusivities were not specified or applied in BESTEST. We will instead treat them as constants for each material, with a representative value for each material (see Table 2-1) drawn from ASHRAE (2005), Chapter 25, Table 7A. As with many of our other assumptions, this limits our conclusions to be for individual representative cases rather than for broad ranges of building constructions. However, the indoor humidity conditions in the building will prove to depend more strongly on infiltration than on moisture transport through the wall, so the diffusivities may be relatively mild assumptions.

### 2.4.3 Convection Mass Transfer

The moisture transport into a solid layer $i$ from an adjacent air space $j$ is

$$\dot{m}_{conv} = h_M A(P_j - P_i) \tag{2.17}$$

where the convection mass transfer coefficient $h_M$ (s/m) in moist air can be approximated from the heat convection coefficient as

$$h_M = \frac{h}{\rho c_{P,air}(Le)^{2/3}} \tag{2.18}$$

with Lewis number $Le \approx 0.845$ (ASHRAE 2005).

### 2.4.4 Infiltration

The rate of change in indoor air moisture mass due to air leakage can be expressed as a difference of mass flow rates between water vapor carried in by outdoor air coming in and water vapor carried out by indoor air, at equal volumetric flow rates of moist air:

$$\dot{m}_{inf} = \dot{m}_{w,out} - \dot{m}_{w,in} = \left(\rho_{w,out} - \rho_{w,in}\right)\dot{V} \tag{2.19}$$

The air infiltration rate is determined by the air change rate $\gamma$ in units of $hr^{-1}$. For convenience, define an infiltration rate in standard units ($s^{-1}$) as $\gamma'_{inf} = \gamma_{inf}/3600$. Then

$$\dot{V} = \gamma'_{inf} V_7 \tag{2.20}$$

Applying the ideal gas law $\rho_w = P/R_w T$,

$$\dot{m}_{inf} = \frac{1}{R_w}\gamma'_{inf}\ V_7 \left(\frac{P_{amb}}{T_{amb}} - \frac{P_7}{T_7}\right) \tag{2.21}$$

### 2.4.5 System of Balance Equations

As with the energy balance, the mass balance can now be expressed as a linear system of equations in the vapor pressures $\{P_1, P_2, \ldots, P_{11}\}$ with the structure shown in Table 2-3 (Ac = Accumulation, Df = Diffusion, Cv = Convection, Inf = Infiltration). The structure is simpler than before due to the lack of radiation and generation terms.

Table 2-3: System of mass balance equations

| | $P_1$ | $P_2$ | $P_3$ | $P_4$ | $P_5$ | $P_6$ | $P_7$ | $P_8$ | $P_9$ | $P_{10}$ | $P_{11}$ | $P'$ | $P_{amb}$ |
|---|---|---|---|---|---|---|---|---|---|---|---|---|---|
| 1 | Ac | Df | | | | | | | | | | Ac | Cv |
| 2 | Df | Ac | Df | | | | | | | | | Ac | |
| 3 | | Df | Ac | Df | | | | | | | | Ac | |
| 4 | | | Df | Ac | Df | | | | | | | Ac | |
| 5 | | | | Df | Ac | Df | | | | | | Ac | |
| 6 | | | | | Df | Ac | Cv | | | | | Ac | |
| 7 | | | | | | Cv | Ac | Cv | | | | Ac | Inf |
| 8 | | | | | | | Cv | Ac | Df | | | Ac | |
| 9 | | | | | | | | Df | Ac | Df | | Ac | |
| 10 | | | | | | | | | Df | Ac | Df | Ac | |
| 11 | | | | | | | | | | | Ac | Ac | |

As with the energy balance equations, the mass balance equations as shown here will be modified slightly in section 2.5 to reflect dehumidification by the air conditioning system.

## 2.5 Including HVAC in Balance Equations

Heating or cooling needed to maintain thermal comfort within a thermostatic setpoint range (by default, the heating and cooling setpoints are $T_{set,H} = 20\,℃$ and $T_{set,C} = 27\,℃$) will be measured by the energy $\dot{E}_{sens}$ needed to counteract the heating or cooling load (W) on the indoor airspace ($> 0$ for heating, $< 0$ for cooling). No computation of associated electrical or chemical energy will be performed, i.e., system efficiency considerations are excluded.

The cooling system also dehumidifies, i.e., removes moisture mass (i.e., latent energy) from the room air according to the Sensible Heat Ratio, $SHR = \dot{E}_{sens}/\dot{E}_{hvac\,total} = \dot{E}_{sens}/(\dot{E}_{sens} + \dot{E}_{lat})$. Thus when the cooling system is delivering a sensible energy flux $\dot{E}_{sens} < 0$, it also delivers a latent energy flux

$$\dot{E}_{lat} = \dot{E}_{sens}\frac{(1 - SHR)}{SHR} \tag{2.22}$$

The determination of SHR will also reflect that A/C systems usually experience latent degradation (i.e., loss of dehumidification power and increased SHR) when operating significantly below their rated capacity.

### 2.5.1 Energy Balance Equations

To include the HVAC effect, the energy balance becomes a 12 x 12 linear system, with $\dot{E}_{sens}$ as the 12th variable, appearing in equation 7 governing the room air (compare to equation (2.12) with infiltration in place of radiation):

$$\rho_7 V_7 c_{P,air} \frac{T_7 - T_7'}{\Delta\tau} = h_6 A_6 (T_6 - T_7) + h_8 A_8 (T_8 - T_7) + \dot{m}_{inf} c_{P,air} (T_{amb} - T_7) + \dot{E}_{sens} \tag{2.23}$$

The 12th equation enforces the setpoints in a two-step process.

1. Solve the 12 x 12 system with row 12 as the setpoint equation $\dot{E}_{sens} = 0$, thereby excluding the HVAC system. If room air is within the comfort range, i.e., $T_{set,H} \leq T_7 \leq T_{set,C}$, then stop; the room air temperature is allowed to float in the current hour.
2. Otherwise, heating or cooling is needed, so solve the system with row 12 as the setpoint equation $T_7 = T_{set,H}$ or $T_7 = T_{set,C}$, whichever was violated. This determines $\dot{E}_{sens}$ in equation 7 as the HVAC input needed to bring the room air temperature back within the setpoint range.

### 2.5.2 Mass Balance Equations

Similarly, dehumidification is addressed in equation 7 governing the moisture mass balance of room air, but only after converting latent energy flux $\dot{E}_{lat}$ to moisture mass rate of change $\dot{m}_{lat}$:

$$\dot{m}_{lat} = \frac{\dot{E}_{lat}}{c_{P,w} T_7} \tag{2.24}$$

where $c_{P,w}$ is the specific heat of water and $T_7$ is the temperature of room air obtained from the energy balance equations for the current hour. This quantity is taken to be independent of the vapor pressure variables, so it is simply a scalar value to be incorporated in the right-hand side term of mass balance equation 7.

## 2.6 Summary

The current chapter has presented the basic nodal model of heat and mass transfers as represented by linear systems of equations in the node temperatures and vapor pressures, including unsteady-state time discretization and the effects of heating and air conditioning.

Chapter 3 describes the numerical procedure to solve these models for the equilibrium temperatures and moisture levels in response to the time series of loads and controls, and shows some illustrative results.

# Chapter 3 Numerical Solution Method and Baseline Results

The temperature and vapor pressure responses of the building elements over time are determined by solving the energy balance and mass balance equations, separately but coupled by the temperature values that appear in the coefficients of the mass balance equations. We will obtain the temperature and vapor pressure profiles over a one-year period by hourly increments, i.e., $\tau = 1, \ldots, 8760$ and $\Delta\tau = 1\ \text{hr} = 3600\ \text{s}$, each hour's results becoming inputs to the succeeding hour's energy and mass balance.

## 3.1 Building and Climate Input Data

The building's structure is determined by the discretization illustrated in Figure 2-1. The physical properties of each material layer (density, thermal conductivity, permeability, etc.) have been specified in Table 2-1.

The set of weather and climatic conditions driving the building temperatures and vapor pressures include ambient air temperature $T_{amb}$, ambient vapor pressure $P_{amb}$, and effective sky and ground temperatures $T_{sky}$ and $T_{gr}$ for radiative heat exchange. These quantities have been extracted or derived from the public TMY2 historical weather data sets (Marion and Urban 1995) for Denver, CO (the original BESTEST location) and Austin, TX. Hourly TMY2 data elements being used include ambient temperature, dewpoint temperature, relative humidity, and cloudiness. From the TMY2 flat file format, we parse $T_{amb}$, the dew point temperature $T_{dp}$, relative humidity $\varphi_{amb}$, and degree of cloud cover $CC$ (ranging from 0 for clear sky to 1 for full overcast).

The ambient vapor pressure (used as input for convection mass transfer and infiltration) is then

$$P_{amb} = \varphi_{amb} \cdot P_{sat}(T_{amb})$$

where $P_{sat}(\cdot)$ is the saturation vapor pressure as a function of temperature. $P_{sat}(T_{amb})$ can easily be obtained by interpolating from a standard temperature table for saturated water.

Per Berdahl and Martin (1984), we obtain an equivalent sky temperature $T_{sky}$ (for use with an effective sky emissivity of $\varepsilon_{sky} = 1$) for long-wave radiative heat exchange with the building envelope as follows (using $T_{amb}$ in K and $T_{dp}$ in ℃):

$$\varepsilon_{clear} = 0.711 + 0.56\left(\frac{T_{dp}}{100}\right) + 0.73\left(\frac{T_{dp}}{100}\right)^2$$

$$T_{clear} = T_{amb}\left(\varepsilon_{clear}^{0.25}\right)$$

$$Ca = 1 + 0.0224\,CC + 0.0035\,CC^2 + 0.00028\,CC^3$$

$$T_{sky} = Ca^{0.25} T_{clear}$$

As stated previously, we have assumed a fixed ground temperature of $T_{gr} = 10$℃.

The hourly short-wave solar radiation intensity on the walls and ceiling is taken from the eQuest building simulation software (Hirsch 2009). eQuest computes insolation from TMY2 data according to solar geometry and cloud cover. For this study, we model a building of appropriate dimensions, location, and orientation in eQuest, run the model, and export the report variables indicating the incident solar radiation intensity on each of the four walls and the roof. Since our nodal model combines the walls and roof into a single one-dimensional element, it remains only to compute the total solar radiation as the sum of radiation intensity times area for each surface, and reduce by a solar reflectivity of 0.2.

It will be clear from context that any of these quantities is specific to the hour $\tau$ in which the balances are currently being solved. The initial temperatures $T'$ for hour $\tau = 1$ are set at 25 ℃ arbitrarily, as the model is not sensitive to the choice. It is more sensitive to the initial vapor pressures $P'$, which are chosen from simulation experience to be consistent with the final pressures at the end of the year.

## 3.2 Air Conditioning Performance Model

As described in section 2.5, sensible cooling rate $\dot{E}_{sens}$ is delivered by the air conditioning system as needed to keep the indoor air temperature from going above the cooling setpoint, and the Sensible Heat Ratio (SHR) determines the accompanying latent

cooling $\dot{E}_{lat}$ and thus the dehumidification. The SHR for a particular A/C unit varies over time with environmental parameters including indoor air temperature and humidity, the outdoor air temperature, and the volumetric airflow rate across the cooling coil. For this study, we model the SHR according to manufacturer's performance data for a conventional residential air conditioner (York 2008). The particular choice of air conditioner affects dehumidification performance, and therefore the applicability of the economizer in climates where it has traditionally been limited by excess humidity. This reduces the breadth of conclusions to be drawn from the results.

On examination, the SHR of the York system depends mainly on the indoor wet bulb temperature (WBT) and outdoor dry bulb temperature (DBT), according to the data points plotted in Figure 3-1. These were generalized by curve-fitting and interpolation. First, exponential functions of the outdoor DBT $T_{amb}$ were curve-fit to the four WBT performance curves, with very close agreement. Then for a given hour, we compute the exponential estimates of SHR given $T_{amb}$ for each of the four WBT curves, and then interpolate to the current WBT using software from the CPAN public software library (Zajac 1998).

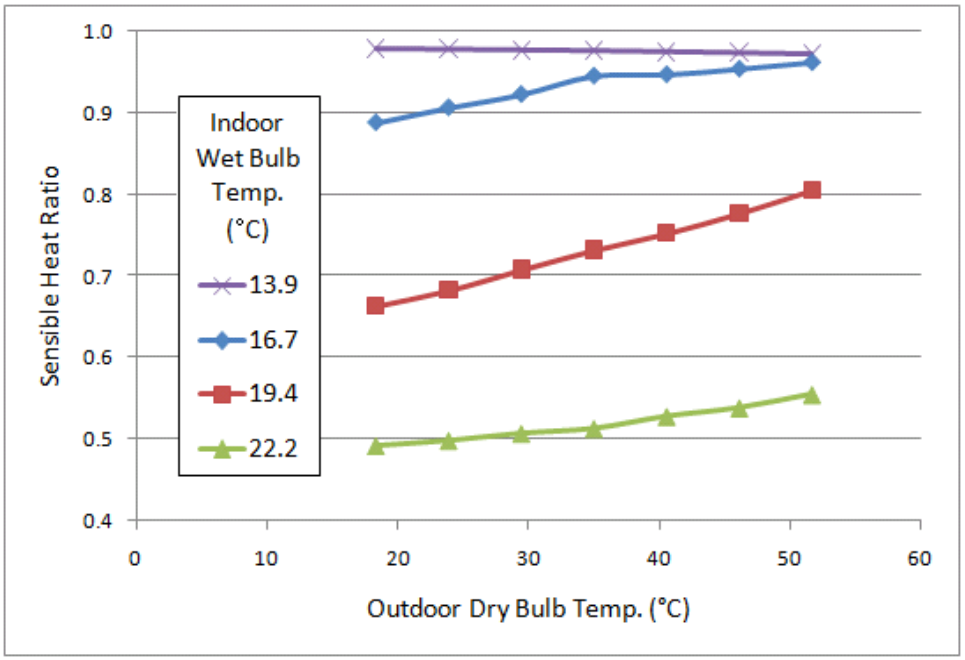


Figure 3-1: Sensible Heat Ratio from manufacturer performance data

One more consideration affects the estimation of SHR. When the A/C system operates below its capacity, it experiences latent degradation, i.e., reduced dehumidification and increased SHR (see, e.g., Henderson and Rengarajan 1996). Henderson et al. (2003) report that the degradation occurs even in systems where the airflow cycles on and off with air conditioning (typically residential), although not as severely as in systems with steady airflow (typically commercial). The field measurements shown there (Figure 8) for residential systems with on/off airflow suggest approximating latent degradation so that SHR is a linear function of the part-load ratio (PLR = load / capacity). That is, SHR is lowest (dehumidification is highest) at peak load, and SHR approaches 1 (no dehumidification) as PLR approaches 0. We will address the impact of this approximation in section 4.4.

To apply latent degradation, we size the capacity of the air conditioner for each test case to meet the design load ($98^{th}$ percentile of hourly cooling loads). Then in each hour, we first compute SHR from the York performance data as above, and modify it for latent degradation according to the PLR for that hour.

## 3.3 Iterative Solution Method

The essential procedure to solve for the hourly temperature and vapor pressure profiles is as follows, beginning at hour $\tau = 1$:

1. In hour $\tau$, construct the energy balance system of equations (left-hand side matrix $A$ and right-hand side vector $v$) per Table 2-2, equations (2.4), (2.5), (2.6), (2.9), and (2.11), and section 2.5.1, substituting the relevant physical constants ($k_i$, $c_{P,i}$, etc.), fixed parameters ($T_{amb}$, $\dot{E}_g$, etc.), and preceding hour's temperatures $T'_1, T'_2, \ldots, T'_{11}$.
2. Solve the linear system $A \cdot T = v$ for the equilibrium solution vector $\{T_1, T_2, \ldots, T_{11}, \dot{E}_{sens}\}$ in the current period.
3. Construct the mass balance system of equations (left-hand side matrix $A_M$ and right-hand side vector $v_M$) per Table 2-3, equations (2.14), (2.15),

(2.16), (2.17), and (2.21), and section 2.5.2, substituting the relevant physical constants ($D_i$, $\xi_i$, etc.), weather parameters ($P_{amb}$, $T_{amb}$), preceding hour's vapor pressures $P'_1, P'_2, \ldots, P'_{11}$, current hour's temperatures $T_1, T_2, \ldots, T_{11}$ and associated vapor saturation pressures $\{P_{sat}(T_i), i = 1, \ldots, 11)\}$.

4. Solve the linear system $A_M \cdot P = v_M$ for the equilibrium solution vector $P = \{P_1, P_2, \ldots, P_{11}\}$ in the current period.
5. Set $\tau = \tau + 1$ and iterate through $\tau = 8760$.

The solution procedure has been implemented in the Perl language, solving the linear systems using code from the CPAN public software library (Pfeifer 2006). Saturation pressures are interpolated from standard values tabulated at range of temperatures. Solving the energy and mass balances for 8760 hours takes about 100 seconds on a 1.8-GHz Windows PC, running Perl inside the Cygwin environment for Unix emulation.

## 3.4 Baseline Results

The discussion here is intended only to show the types of information to be obtained from the test cases. Chapter 4 will introduce the opportunity for free cooling with outside air and give results by building construction, location, economizer parameters, etc.

HVAC consumption results are shown in Table 3-1; recall that the heating and cooling loads are given for the indoor air space, without considering fuel source or system efficiency. The table indicates that:

- Heavier construction reduces heating load modestly and cooling load considerably.
- Cooling in Denver is very low for the light building and negligible for the heavy building, and the incidence of excessive indoor relative humidity ($\varphi_6$) in the drier climate of Denver is very small. The heavier construction reduces hours of excessive humidity in both locations.

- The effect of construction on floating hours (no heating or cooling needed, indoor temperature can float within indoor comfort range) depends on location. The fewer floating hours for heavier construction in Austin is apparently due to the building holding stored daytime heat longer into the night, heating the room air.

The annual profile of temperatures is illustrated in Figure 3-2 for the Austin location, showing the ambient air temperature and the room air temperature (in K) for both building constructions. The effect of the thermostatic comfort range (293 K – 300 K) is clearly visible, as well as the effect of the heavier construction in damping the temperature swings of the indoor air. A similar effect governs the annual profile of relative humidities, as shown in Figure 3-3.

Table 3-1: Baseline heating and cooling loads

| | | *Hours (annual=8760)* | | | *Hours (annual=8760)* | | *Loads (kWh)* | |
|---|---|---|---|---|---|---|---|---|
| *Location* | *Construction* | *Float* | *Heating* | *Cooling* | *RH ($\varphi_6$) $\leq 0.7$* | *RH ($\varphi_6$) $> 0.7$* | *Heating kWh* | *Cooling kWh* |
| Austin | Light | 3979 | 2247 | 2534 | 8480 | 280 | 1922 | -1625 |
| Austin | Heavy | 3892 | 2082 | 2786 | 8755 | 5 | 1608 | -1334 |
| Denver | Light | 2869 | 5260 | 631 | 8748 | 12 | 6495 | -339 |
| Denver | Heavy | 3158 | 5372 | 230 | 8760 | 0 | 6485 | -77 |

Figure 3-4 focuses in on the temperatures in June-August, showing that there are many periods when the room temperature is at or near the cooling setpoint, activating the air conditioner, even when the ambient air temperature is less, and could be used for free cooling.

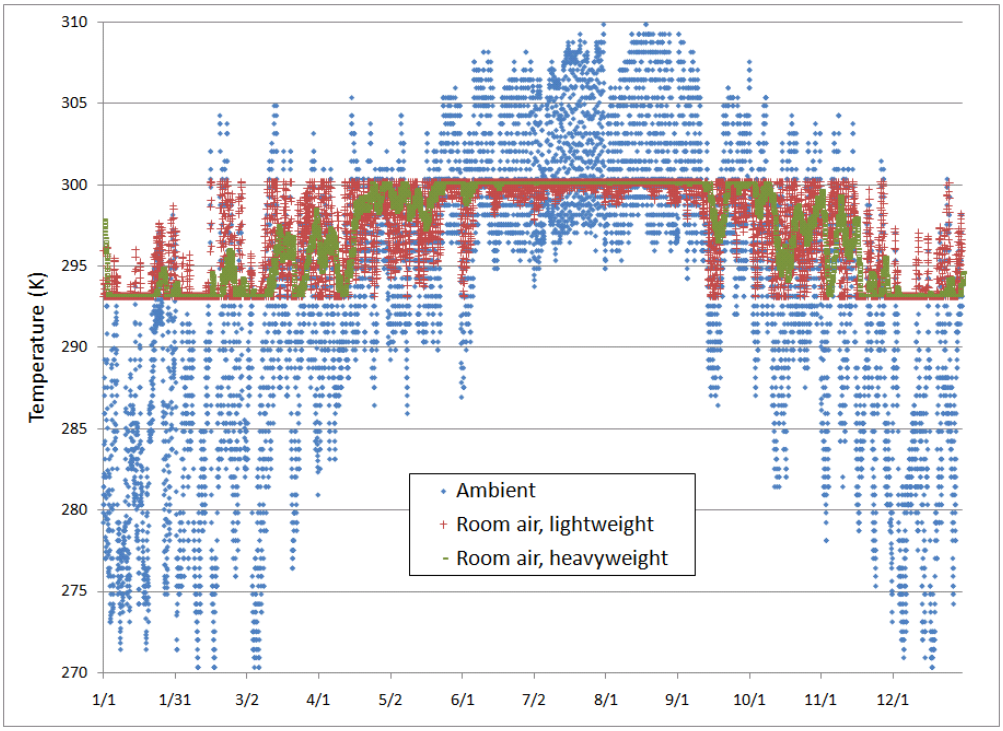


Figure 3-2: Hourly temperatures for Austin location

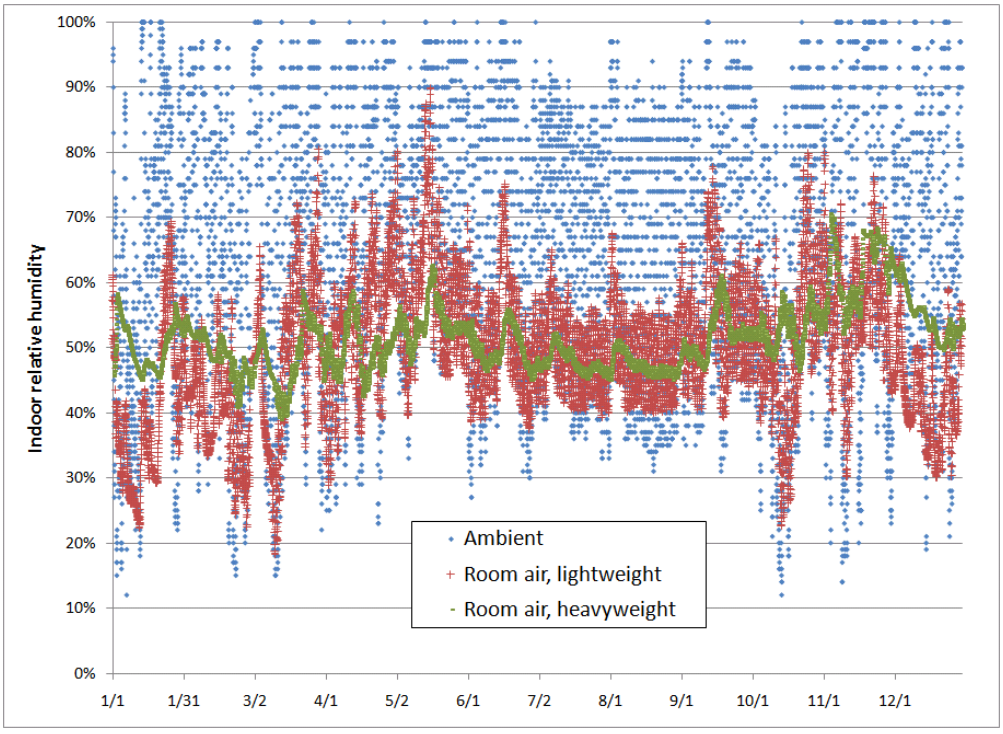


Figure 3-3: Hourly relative humidities for Austin location

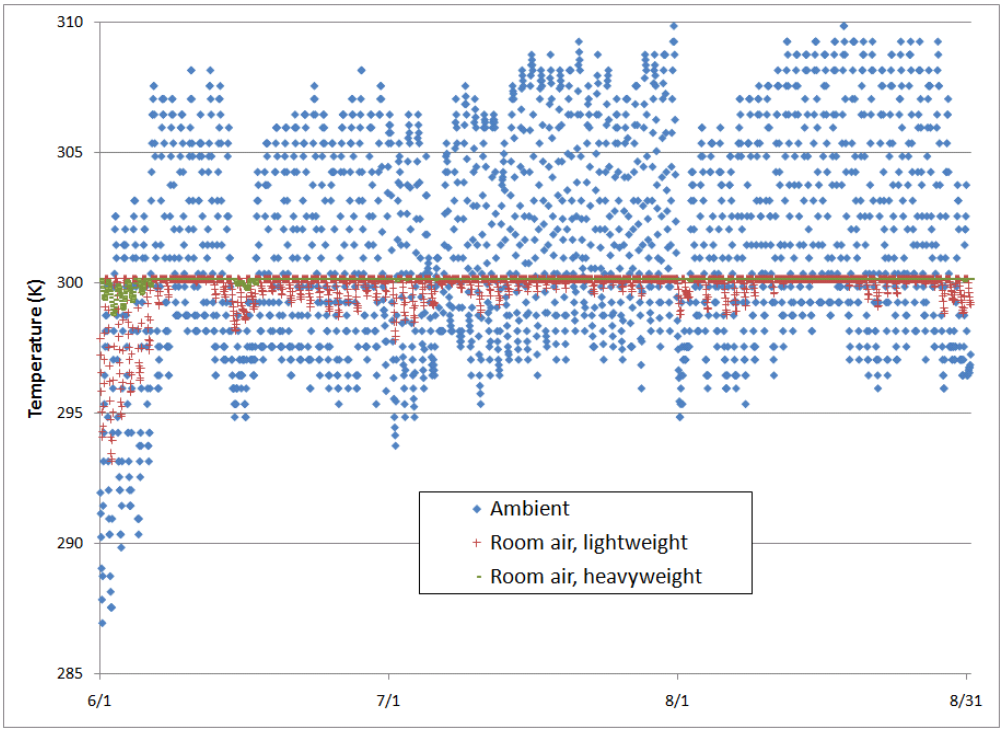


Figure 3-4: Hourly temperatures, Austin, June-August

# Chapter 4 Free cooling by economizer

Systems that introduce extra outdoor air to cool the indoor air in place of running the A/C system are generally known as economizers. We previously defined our buildings to have a constant infiltration of $\gamma_{inf} = 0.5$ ACH to represent the effects of leakage, wind, pressure difference vs. ambient, etc. We now assume that there is an additional air intake and air exhaust, driven by a variable-speed or on/off cycling fan to bring about an additional exchange at rate $\gamma_{econ}$. $\gamma_{econ}$ will be determined by control logic seeking a high free cooling benefit, up to a limit $\gamma_{max}$ representing the limits of the economizer fan. The overall effect is then $\gamma_{tot} = \gamma_{inf} + \gamma_{econ}$.

These assumptions are highly simplified, ignoring variation in the infiltration rate due to changing wind and weather, indoor temperature, and interactions between infiltration and ventilation. The control logic will also be based on simplified heuristics rather than optimization, for both conventional instantaneous economizer control and forecast-based control. The purpose is to illustrate the potential for different economizer control modes within the limited accuracy of our simplified building energy model, ideally motivating more accurate analyses and control approaches in the future.

We present first the instantaneous economizer control and then the forecast-based control.

## 4.1 Instantaneous Economizer Control

A control in this situation consists of a value of $\gamma_{econ}$ for each hour of the annual simulation. If $\gamma_{econ} = 0$, the economizer is turned off because free cooling is not available or not beneficial (due to excess humidity, for example). We will ultimately manage the economizer by a combination of instantaneous and forecast-based values, i.e., $\gamma_{econ} = \gamma_{inst} + \gamma_{fcast}$, but for now we hold $\gamma_{fcast} = 0$ and address $\gamma_{inst}$.

In each hour, after solving for $\{T_1, T_2, \dots, T_{11}, \dot{E}_{sens}\}$ by the two-step process of section 2.5.1 (first solve without a setpoint; if a setpoint is violated, augment the matrix to enforce it and re-solve):

1. Check whether $\dot{E}_{sens} < 0$ (cooling needed) and $\Delta T = T_{amb} - T_7 < -\varepsilon$ (outdoor air cooler than indoor, by at least some small margin $\varepsilon > 0$). If so, free cooling is available; otherwise set $\gamma_{inst} = 0$.
2. Estimate the free cooling rate already in effect due to infiltration as

$$\dot{E}_{inf} = \gamma_{inf} \frac{\rho_{air} V_7 c_{P,air} \Delta T}{\Delta \tau}$$

3. Estimate the economizer control needed to replace the HVAC cooling demand (within the fan power limit) as

$$\gamma_{inst} = \min \left\{ \gamma_{inf} \frac{\dot{E}_{sens}}{\dot{E}_{inf}}, \gamma_{max} \right\}$$

4. Re-solve the energy balance equations with $\gamma_{inst} + \gamma_{inf}$ in place of $\gamma_{inf}$ and the cooling setpoint constraint in place ($T_7 = T_{set,C}$).
5. Due to the approximate nature of the estimated free cooling effect, overcooling may have occurred, so that the new solution includes heating ($\dot{E}_{sens} > 0$) in order to meet the cooling setpoint constraint. If so, iterate step 4 while decreasing $\gamma_{inst}$ in increments 10% of its original value in step 3, until no heating is called for.

Thus when free cooling is available and wanted, some portion of the cooling demand is met with outdoor air at an airflow rate $\gamma_{inst}$ air changes per hour, replacing cooling load that would otherwise have been met by A/C power. In this approach, the economizer is used only to cool the room down to the cooling setpoint $T_{set,C}$ (e.g., 27 ℃) and not further. The opportunity to cool further now, to reduce A/C energy consumption in the succeeding hours when free cooling may not be available, is lost.

## 4.2 Instantaneous Control with Humidity Constraint

As will be shown shortly, in many periods the humidity outdoor air is humid enough that its moisture content, introduced into the room air by the economizer, increases room humidity $\varphi_7$ well above 70%, which we take to be the comfort limit.

Further, free cooling is substituting for A/C operation and its associated dehumidification, exacerbating the humidity increase.

We could mitigate this by adding a dedicated humidifier, removing moisture mass to meet a precise constraint on $\varphi_7$, just like we use the A/C system to remove sensible energy to meet setpoint constraints. Alternatively, we could iterate between the energy balance and mass balance systems for a given hour to solve exactly for $\gamma_{inst}$ with respect to the constraint on $\varphi_7$.

However, in keeping with the approximate and heuristic nature of the overall model, we take a simpler approach. A relative humidity of $\varphi_7 = 0.7$ at the cooling setpoint of 27 ℃ implies a vapor pressure of $2520\ Pa$. Based on trials of how many hours of excess humidity would result, we lock out the economizer (i.e., set $\gamma_{inst} = 0$) if the room air is already near the limit ($P_7' > 2400\ Pa$) and the outdoor air is moist ($P_{amb} > 2400\ Pa$), or if the outdoor air is very moist ($P_{amb} > 2700\ Pa$). Note that the ambient air is judged not by relative humidity but by vapor pressure, which bears more directly on the rate of moisture gain from outside.

Table 4-1 shows the effect of the economizer on A/C utilization, both in simple humidity-unconstrained operation and with the humidity lockout. The results include test cases for $\gamma_{max} = 10\ ACH$ and $\gamma_{max} = 50\ ACH$. The economizer airflow rate of 10 ACH, applied to the indoor air volume and after unit conversion, corresponds to 360 liters per second (762 cubic feet per minute), which is a moderate-to-high fan airflow rate for a residential system. This seems reasonable because the economizer fan in this system doesn't have to overcome the pressure drop of pushing through a cooling coil or an extensive duct system. The higher level of 50 ACH is intended to determine whether the economizer airflow rate is a limiting factor.

We observe that:

- The instantaneous economizer control never affects heating in number of hours or total load. (There may be a modest opportunity for free heating, but this analysis doesn't look for it.)

- Cooling load is reduced to a greater extent in the building with greater thermal mass. The impacts are:
    - Austin: lightweight, 4-6%; heavyweight 15-25%
    - Denver: lightweight, 10-14%; heavyweight 27-32%, although the impact is small in magnitude in the relatively cool climate
- Humidity lockout is significant in Austin and has no effect in the relatively dry climate of Denver. In Austin, it affects both cooling load reduction and the number of hours violating the humidity comfort condition; with lockout, the number of hours made over-humid by the economizer is reduced by more than half.

Table 4-1: HVAC operation with instantaneous economizer control

| | | | | *Hours (annual=8760)* | | | | *Hours* | | *Loads (kWh)* | | |
|---|---|---|---|---|---|---|---|---|---|---|---|---|
| *Location* | *Const.* | *Humidity rule* | *$\gamma_{max}$ (ach)* | *Float* | *Heating* | *HVAC Cooling* | *Free Cooling* | *RH ($\varphi_6$) $\leq 0.7$* | *RH ($\varphi_6$) $> 0.7$* | *Heating kWh* | *Cooling kWh* | *Cooling % Chng* |
| Austin | Light | Free | 0 | 3979 | 2247 | 2534 | 0 | 8480 | 280 | 1922 | -1625 | |
| Austin | Light | Free | 10 | 3979 | 2247 | 1844 | 690 | 8254 | 506 | 1922 | -1546 | -5% |
| Austin | Light | Free | 50 | 3979 | 2247 | 1844 | 690 | 8233 | 527 | 1922 | -1524 | -6% |
| Austin | Light | Lockout | 0 | 3979 | 2247 | 2534 | 0 | 8480 | 280 | 1922 | -1625 | |
| Austin | Light | Lockout | 10 | 3979 | 2247 | 2046 | 488 | 8375 | 385 | 1922 | -1563 | -4% |
| Austin | Light | Lockout | 50 | 3979 | 2247 | 2048 | 486 | 8363 | 397 | 1922 | -1544 | -5% |
| Austin | Heavy | Free | 0 | 3892 | 2082 | 2786 | 0 | 8755 | 5 | 1608 | -1334 | |
| Austin | Heavy | Free | 10 | 3892 | 2082 | 1576 | 1210 | 8513 | 247 | 1608 | -1059 | -21% |
| Austin | Heavy | Free | 50 | 3892 | 2082 | 1576 | 1210 | 8419 | 341 | 1608 | -1005 | -25% |
| Austin | Heavy | Lockout | 0 | 3892 | 2082 | 2786 | 0 | 8755 | 5 | 1608 | -1334 | |
| Austin | Heavy | Lockout | 10 | 3892 | 2082 | 1949 | 837 | 8608 | 152 | 1608 | -1138 | -15% |
| Austin | Heavy | Lockout | 50 | 3892 | 2082 | 1958 | 828 | 8583 | 177 | 1608 | -1104 | -17% |
| Denver | Light | Free | 0 | 2869 | 5260 | 631 | 0 | 8748 | 12 | 6495 | -339 | |
| Denver | Light | Free | 10 | 2869 | 5260 | 421 | 210 | 8743 | 17 | 6495 | -305 | -10% |
| Denver | Light | Free | 50 | 2869 | 5260 | 421 | 210 | 8742 | 18 | 6495 | -292 | -14% |
| Denver | Light | Lockout | 0 | 2869 | 5260 | 631 | 0 | 8748 | 12 | 6495 | -339 | |
| Denver | Light | Lockout | 10 | 2869 | 5260 | 421 | 210 | 8743 | 17 | 6495 | -305 | -10% |
| Denver | Light | Lockout | 50 | 2869 | 5260 | 421 | 210 | 8742 | 18 | 6495 | -292 | -14% |
| Denver | Heavy | Free | 0 | 3158 | 5372 | 230 | 0 | 8760 | 0 | 6485 | -77 | |
| Denver | Heavy | Free | 10 | 3158 | 5372 | 125 | 105 | 8760 | 0 | 6485 | -56 | -27% |
| Denver | Heavy | Free | 50 | 3158 | 5372 | 125 | 105 | 8760 | 0 | 6485 | -52 | -32% |
| Denver | Heavy | Lockout | 0 | 3158 | 5372 | 230 | 0 | 8760 | 0 | 6485 | -77 | |
| Denver | Heavy | Lockout | 10 | 3158 | 5372 | 125 | 105 | 8760 | 0 | 6485 | -56 | -27% |
| Denver | Heavy | Lockout | 50 | 3158 | 5372 | 125 | 105 | 8760 | 0 | 6485 | -52 | -32% |

## 4.3 Forecast-Based Economizer Control

To illustrate the opportunity for forecast-based free cooling, consider the hourly temperatures (room air, its adjacent building layers, and ambient, i.e., $\{T_6, T_7, T_8, T_{amb}\}$) shown in Figure 4-1 for a summer week with the instantaneous economizer in operation. While the ambient temperature falls below the cooling setpoint at night, the room air temperature $T_7$ mainly stays at the cooling setpoint ($27\,℃ = 300.15\,K$). Further, the adjacent wall layer temperature $T_6$ is raised above the setpoint during the day due to conduction inward of heat gained from outside by convection and radiation. This raises the floor temperature $T_8$ by radiation, and both layers heat the room air by convection, increasing the cooling load.

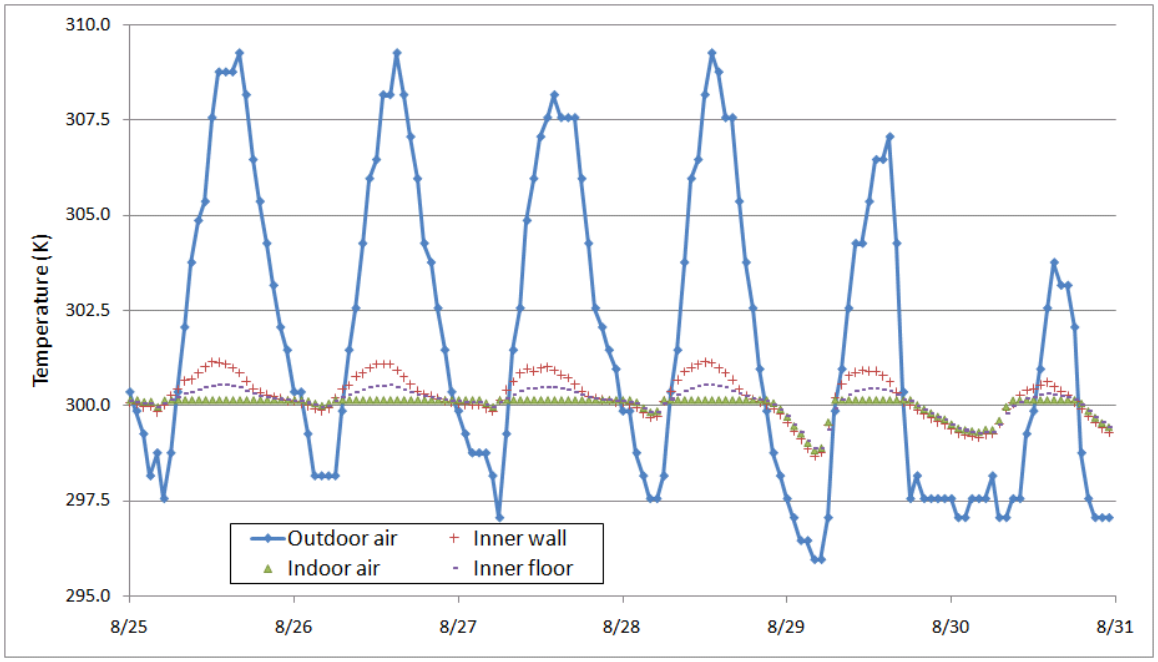


Figure 4-1: Summer building element temperatures with instantaneous economizer

It would be better to cool the room air and the adjacent building layers below the cooling setpoint during the overnight periods of cool outdoor air, so that they can float upwards during the day, until they finally reach the cooling setpoint and require A/C operation, but at a reduced total load for the day.

In some seasons however, the cool overnight may be followed by a cool, overcast day in which the economizer would *overcool* the interior elements down near the heating setpoint, creating an otherwise unnecessary heating load. To illustrate the best-case potential for applying additional free cooling, we will model the situation where the economizer controller has access to an accurate weather forecast and enough of a building energy model to produce an accurate prediction of upcoming hour-by-hour cooling loads and building element temperatures. For simplicity and to identify the best-case benefits to be achieved from a very accurate forecast, we simulate the prediction of loads by actually iterating backward through the hours of the year and computing a forecast-based economizer airflow air change rate $\gamma_{fcast}$ in hour $\tau$ as a function of the room air temperatures and cooling loads in hours $\{\tau + 1, \tau + 2, \dots, \tau + 24\}$.

### 4.3.1 Forecast-Based Economizer Airflow for a Single Hour

Before stating the entire algorithm iterating through the full year, we first explain the process for a single hour. For the building envelopes studied here, the middle layer of the wall is strongly insulating, and the flooring also rests on a strongly insulating floor insulation layer. Thus, we initially estimate the effect of $\gamma_{fcast}$ on the building by assuming that the heat transfer from outdoor air to indoors goes entirely into the room air and inner layers of walls and floor. These elements have combined thermal mass

$$(mc_P)_{comb} = \sum_{j \epsilon \{room\ air;\ inner\ layers\ of\ wall\ and\ floor\}} \rho_j V_j c_{P,j}$$

These wall and floor layers include nodes 6-8 and the inner portion of nodes 5 and 9, excluding the outer portion of nodes 5 and 9 consisting of insulation materials, per the space discretization in Figure 2-1.

The process in hour $\tau$ is then:

1. If this is a heating or cooling hour ($\dot{E}_{sens} \neq 0$), set $\gamma_{fcast}^{\tau} = 0$ and re-initialize $T_{min} = T_{set,C}$. No forecast-based cooling is needed. (If heating, this is obvious. If cooling, then the instantaneous economizer can be expected to operate as much as would be useful up to the fan power limit, without needing

to forecast future conditions.)

Set a flag $f_{cool} = 1$ if it's a cooling hour, to indicate cooling we hope to avoid. Otherwise set $f_{cool} = 0$. Iterate to hour $\tau - 1$.

2. For hours without heating or cooling ($\dot{E}_{sens} = 0$), set

$$T_{min} = \min\left(T_{min}, T_{set,C}\right)$$

As we step backwards in time, $T_{min}$ will track the lowest upcoming room temperature within the forecast window. It will be used to avoid overcooling the room now so that the room temperature would fall below the heating setpoint $T_{set,H}$ later and require additional heating.

3. If the next cooling hour is at least 24 hours ahead, set $\gamma_{fcast}^{\tau} = 0$ and iterate to hour $\tau - 1$. The impact of forecasting longer than one day ahead is considered too attenuated to be of value.
4. Check whether free cooling is available and wanted, i.e., if
   a. $f_{cool} = 1$, i.e., the next HVAC demand is for cooling, and
   b. $\Delta T_{inf} = T_{amb} - T_7 < -\varepsilon$ (outdoor air cooler than indoor, by at least some small margin $\varepsilon > 0$), and
   c. $T_{min} > T_{set,H}$, i.e., the lowest temperature in the upcoming time window has room to be decreased by economizer operation in this hour, without creating a heating demand.

   If not, set $\gamma_{fcast}^{\tau} = 0$ and iterate to hour $\tau - 1$.
5. Compute the desired change for room temperature in this hour by economizer as $\Delta T_{target} = T_{min} - T_{set,H}$
6. Estimate the economizer airflow needed from an approximate energy balance of economizer vs. accumulation:

$$\gamma_{fcast}^{\tau} \frac{\rho_{air} V_7 c_{P,air} \Delta T_{inf}}{\Delta\tau} = \frac{(mc_P)_{comb} \Delta T_{target}}{\Delta\tau}$$

$$\Rightarrow \qquad \gamma_{fcast}^{\tau} = \frac{(mc_P)_{comb}}{\rho_{air} V_7 c_{P,air}} \frac{\Delta T_{target}}{\Delta T_{inf}}$$

7. Incorporate the fan power constraint:

$$\gamma_{fcast}^{\tau} = \min\{\gamma_{fcast}^{\tau}, \gamma_{max}\}$$

8. Iterate to hour $\tau - 1$.

### 4.3.2 Multi-Phase Algorithm for Forecast-Based Economizer Airflow

After completing the reverse iteration and computing $\gamma_{fcast}$ for each hour, we will then proceed forward in time once again, solving the energy and mass balance models in each hour. That stage of the algorithm (Phase III) is mainly the same as in section 4.1, except with combined air exchange rate $\gamma_{inf} + \gamma_{fcast}$ in place of baseline infiltration rate $\gamma_{inf}$.

Phase I. Solve the energy and mass balances for the year forward in time, with the instantaneous economizer available up to an airflow of $\gamma_{max}$ in each hour, as in section 4.1 (or 4.2, if humidity lockout is desired).

Phase II. Iterate backward in time to determine initial values of $\gamma_{fcast}$ for each hour per section 4.3.1.

Phase III. Iterate forward in time again. In each hour, solve first without $\gamma_{inst}$ and then with it, as in Phase I.

III.1. If humidity lockout is active and applies to hour $\tau$ due to humid conditions, override the forecast-based control by setting $\gamma_{fcast} = 0$.

III.2. Solve the energy balance as usual, but with infiltration rate $\gamma_{inf} + \gamma_{fcast}$ in place of $\gamma_{inf}$. As in section 2.5.1, solve first without a setpoint constraint (floating temperature), and then if a setpoint is violated, add it to the linear system and re-solve.

III.3. If overcooling has occurred ($\dot{E}_{sens} > 0$), decrease $\gamma_{fcast}$ in increments of 10% of its original value and repeat step III.2 until the overcooling is eliminated.

III.4. Check whether $\dot{E}_{sens} < 0$ (A/C needed) and $\Delta T = T_{amb} - T_7 < -\varepsilon$ (outdoor air cooler than indoor, by at least some small margin

$\varepsilon > 0$). If so, free cooling is available; otherwise set $\gamma_{inst} = 0$ and iterate to Phase I for hour $\tau + 1$.

III.5. Estimate the free cooling rate already in effect due to infiltration as

$$\dot{E}_{inf} = (\gamma_{inf} + \gamma_{fcast}) \frac{\rho_{air} V_7 c_{P,air} \Delta T}{\Delta \tau}$$

III.6. Estimate the economizer control needed to replace the HVAC cooling demand (within the fan power limit) as

$$\gamma_{inst} = \min \left\{ \frac{\dot{E}_{sens}}{\dot{E}_{inf}}, \gamma_{max} \right\}$$

III.7. Re-solve the energy balance equations as in step III.2 but with $\gamma_{inf} + \gamma_{fcast} + \gamma_{inst}$ in place of $\gamma_{inf}$.

III.8. If overcooling has occurred ($\dot{E}_{sens} > 0$), decrease $\gamma_{inst}$ in increments of 10% of its original value from step III.6 and repeat step III.7 until the overcooling is eliminated.

III.9. Solve the moisture mass balance, based on the final temperature solution from step III.8.

III.10. Iterate to Phase I for hour $\tau + 1$.

### 4.3.3 Simulation results for forecast-based economizer

The first set of results for the forecast-based economizer is presented in Table 4-2. For this run, the results were essentially identical for maximum airflow rate of 10 or 50 ach, so only the results for $\gamma_{max} = 10$ are presented. Also, there were initially many more hours of free cooling rather than A/C cooling, causing a large increase in the number of hours over 70% indoor humidity. To restrain this effect, the vapor pressure criteria for humidity lockout have been broadened. The rule for lockout when indoor and outdoor air are already moist is now $P_7' > 2200\ Pa$ and $P_{amb} > 2200\ Pa$, in place of the previous threshold of $2400\ Pa$. Also, the criterion for lockout when the outdoor air is very moist is now $P_{amb} > 2500\ Pa$, in place of the previous threshold of $2700\ Pa$. The new values were chosen experimentally so that the heuristic would restrict hours of

excess humidity to about the same level as the previous values yielded for the instantaneous economizer control.

We observe the following:

- When humidity lockout is not in effect, we obtain relatively large reductions in total cooling load for both buildings in both locations, but in Austin the number of hours of excess indoor humidity is very large, about 2000 hours per year.
    - In Austin, cooling load is reduced by 14-48% depending on building construction.
- The humidity lockout in Austin is very effective in reducing excess humidity hours. However, it achieves little cooling load savings relative to the instantaneous economizer control.
    - For the heavyweight case, load is reduced by 20%, compared to a 15% reduction in load and approximately the same number of excess humidity hours with the instantaneous economizer (cf. Table 4-1).
    - For the lightweight case, the excess humidity hours are greatly increased, in exchange for a very modest improvement in total cooling load.
- Humidity lockout in the relatively dry Denver climate had no impact and was not needed.
- The forecast-based economizer slightly increases the heating load for the lightweight building. The economizer airflow rate is scaled down in each hour to prevent overcooling and resulting heating load in that hour, but due to the heuristic nature of the forecast-based control, it may overcool so as to cause heating demand in subsequent hours.

Table 4-2: Results for forecast-based economizer control

| | | | | Hours (annual=8760) | | | | Hours | | Loads (kWh) | | |
|---|---|---|---|---|---|---|---|---|---|---|---|---|
| Location | Const. | Humidity rule | $\gamma_{max}$ (ach) | Float | Heating | HVAC Cooling | Free Cooling | RH ($\varphi_6$) $\leq 0.7$ | RH ($\varphi_6$) $> 0.7$ | Heating kWh | Cooling kWh | Cooling % Chng |
| Austin | Light | Free | 0 | 3979 | 2247 | 2534 | 0 | 8480 | 280 | 1922 | -1625 | |
| Austin | Light | Free | 10 | 2548 | 2333 | 1730 | 2149 | 6724 | 2036 | 1929 | -1396 | -14% |
| Austin | Light | Lockout | 0 | 3979 | 2247 | 2534 | 0 | 8480 | 280 | 1922 | -1625 | |
| Austin | Light | Lockout | 10 | 3229 | 2331 | 2170 | 1030 | 7839 | 921 | 1929 | -1515 | -7% |
| Austin | Heavy | Free | 0 | 3892 | 2082 | 2786 | 0 | 8755 | 5 | 1608 | -1334 | |
| Austin | Heavy | Free | 10 | 4046 | 2082 | 1114 | 1518 | 6886 | 1874 | 1608 | -697 | -48% |
| Austin | Heavy | Lockout | 0 | 3892 | 2082 | 2786 | 0 | 8755 | 5 | 1608 | -1334 | |
| Austin | Heavy | Lockout | 10 | 4044 | 2082 | 2036 | 598 | 8588 | 172 | 1608 | -1072 | -20% |
| Denver | Light | Free | 0 | 2869 | 5260 | 631 | 0 | 8748 | 12 | 6495 | -339 | |
| Denver | Light | Free | 10 | 2298 | 5365 | 387 | 218 | 8709 | 51 | 6508 | -267 | -21% |
| Denver | Light | Lockout | 0 | 2869 | 5260 | 631 | 0 | 8748 | 12 | 6495 | -339 | |
| Denver | Light | Lockout | 10 | 2298 | 5365 | 387 | 218 | 8709 | 51 | 6508 | -267 | -21% |
| Denver | Heavy | Free | 0 | 3158 | 5372 | 230 | 204 | 8760 | 0 | 6485 | -77 | |
| Denver | Heavy | Free | 10 | 3127 | 5374 | 0 | 204 | 8760 | 0 | 6485 | 0 | -100% |
| Denver | Heavy | Lockout | 0 | 3158 | 5372 | 230 | 0 | 8760 | 0 | 6485 | -77 | |
| Denver | Heavy | Lockout | 10 | 3127 | 5374 | 0 | 33 | 8760 | 0 | 6485 | 0 | -100% |

For these test cases, we conclude that heavyweight construction with high levels of thermal and moisture mass are important if the forecast-based economizer is to meet or exceed the cooling load reduction and thermal comfort performance of the instantaneous economizer control, but even so, it shows little incremental benefit in these test cases.

## 4.4 Sensitivity to Latent Degradation

We now inquire whether the excessive indoor humidity often associated with the forecast-based economizer control is significantly due to latent degradation at part-load A/C conditions, as discussed in section 3.2. If so, then we could consider whether a variable-capacity air-conditioning system running at a steady cooling rate would avoid the latent degradation, dehumidify better over the full range of cooling load conditions, and maintain a lower hourly profile of indoor humidity. The effects of operating with or without latent degradation are shown in Table 4-3 for $\gamma_{max} = 10$.

Table 4-3: Effect of latent degradation on forecast-based economizer performance

| | | | | Hours (annual=8760) | | | | Hours | | Loads (kWh) | | |
|---|---|---|---|---|---|---|---|---|---|---|---|---|
| Location | Const. | Humidity rule | Latent degradation | Float | Heating | HVAC Cooling | Free Cooling | RH ($\varphi_6$) $\leq 0.7$ | RH ($\varphi_6$) $> 0.7$ | Heating kWh | Cooling kWh | Cooling % Chng |
| Austin | Light | Free | Yes | 2548 | 2333 | 1730 | 2149 | 6724 | 2036 | 1929 | -1396 | |
| Austin | Light | Free | No | 2548 | 2333 | 1730 | 2149 | 6848 | 1912 | 1929 | -1396 | 0% |
| Austin | Light | Lockout | Yes | 3229 | 2331 | 2170 | 1030 | 7839 | 921 | 1929 | -1515 | |
| Austin | Light | Lockout | No | 3210 | 2331 | 2164 | 1055 | 7884 | 876 | 1929 | -1511 | 0% |
| Austin | Heavy | Free | Yes | 4046 | 2082 | 1114 | 1518 | 6886 | 1874 | 1608 | -697 | |
| Austin | Heavy | Free | No | 4046 | 2082 | 1114 | 1518 | 7061 | 1699 | 1608 | -697 | 0% |
| Austin | Heavy | Lockout | Yes | 4044 | 2082 | 2036 | 598 | 8588 | 172 | 1608 | -1072 | |
| Austin | Heavy | Lockout | No | 4047 | 2082 | 2031 | 600 | 8636 | 124 | 1608 | -1067 | 0% |

The results show a negligible effect on heating and cooling load and a very modest effect on annual hours of excess indoor humidity. Therefore these cases do not support the proposal for variable-capacity residential air conditioning in relation to the economizer benefits.

# Chapter 5 Discussion and Conclusions

In this thesis, we have investigated the potential for increasing the range of conditions in which an economizer would be beneficial for residential free cooling. We have simulated the use of an idealized forecast of upcoming weather conditions to precool a home overnight, often down to a lower limit at the thermostat heating setpoint. The forecast is used to avoid conditions where the indoor air cools further before it warms up again, creating a heating load that could have been avoided. This chapter reviews the findings of the study and considers other implications and directions for further study.

## 5.1 Review of Analysis Results

As found previously in the literature, the usefulness of the economizer is severely limited by humidity in the outdoor air, which often leads to excessive humidity in the indoor air. The outdoor air may already contain a high moisture level (i.e., water vapor partial pressure), especially in hot and humid climates like Austin, which implies higher relative humidity when the air is cool enough to be useful. Also, when free cooling by the economizer replaces sensible cooling by the home air conditioner, the idled air conditioner is not performing latent cooling, i.e., dehumidification. The combined effect can be severe. Using the forecast-based economizer in the building with heavy construction and without concern for indoor humidity, i.e., no humidity lockout, reduces estimated annual cooling load by 48%, but hours with excessive indoor relative humidity (over 70%) increase from 5 to 1874, which is 21% of the year. Adding the humidity lockout keeps the hours of excessive indoor humidity to 172, but the savings in annual cooling load is then only 20%. In the same scenario, simply using the instantaneous economizer control (no forecasting; simply use outside air whenever it's cool enough in that hour and cooling is needed) saves 15% of annual cooling load, with 152 hours of excessive indoor humidity. Thus, the forecasting approach saves only minimally on annual cooling load, even before considering power that would be consumed by the

economizer fan. The results for the light-construction house are even less favorable to the forecasting approach.

In the less humid climate in Denver, the forecasting approach appears to be more valuable. With equivalent limits of 10 ACH on economizer fan airflow rate, the forecasting approach saves 21% of annual cooling load, vs. 10% for the instantaneous economizer control, for light construction, and 100% (forecasting) vs. 27% (instantaneous) for heavy construction. However, the absolute cooling load in Denver is small enough that the actual energy savings for this house model would not justify investing in the forecast-based economizer capability. Further studies can consider larger house models with greater annual cooling loads and warmer dry climates, which may identify scenarios where the savings justify the investment. In addition, dry climates like Denver are already known to be relatively favorable for economizer use, so we have not achieved the goal of expanding the range of climates where economizers are worthwhile.

We also considered how a variable-capacity residential air conditioner might lower the overall profiles of indoor relative humidity in the simulations by avoiding latent degradation (loss of dehumidification effects at part-load conditions). However, the benefits of this approach were not significant.

## 5.2 Impacts of Key Parameters and Modeling Assumptions

### 5.2.1 Thermal and Moisture Mass

It is apparent that thermal and moisture mass play a major role in economizer effectiveness, both forecast-based and instantaneous. A larger thermal mass stores more cooling relative to the indoor air and the external thermal loads, and it smoothes the indoor temperature variations due to day/night variation. This makes the precooling effect of the economizer more effective in all modes: instantaneous, forecasting, and incremental benefit of forecast vs. instantaneous. A larger moisture mass can absorb more water vapor coming in through the economizer, which may allow the use of free cooling for overnight hours while keeping indoor relative humidity within bounds, until the air conditioning comes on later in the day and provides some dehumidification.

Many of the assumptions made in setting up the parameters of the house construction and the modeling approach should have their main impact on economizer effectiveness via the thermal and moisture mass. The materials making up the building envelope and their physical properties (thickness, density, specific heat, thermal conductivity, moisture capacity) contribute in a straightforward way to the thermal and moisture mass of the individual layers and the combined envelope.

These properties are also important in determining the thermal and diffusion resistance of the envelope, which will have an important effect on cooling load whether or not the economizer is in use, regardless of control algorithm. However, the overall thermal resistance seems likely to have only a secondary effect on the relative benefits of different economizer approaches.

Thus, to study the effects of varying physical materials and dimensions, it may be worthwhile to aggregate their parameters into characteristic values for thermal and moisture mass. The question then would be whether the characteristic values correlate well with economizer control algorithm performance, without additional reference to the underlying parameters. If so, it would simplify further studies of how economizer algorithm performance varies with building structure. These characteristic values may also account for the thermal and moisture storage properties of the contents of the house such as carpets and furnishings.

### 5.2.2 Building Design and Layout

The major simplifying assumptions made on the building structure were first, a single room, and second, the walls and ceiling behaving as a combined surface with uniform heating and cooling loads and simple one-dimensional heat and moisture transport. These assumptions are clearly connected; in a real home with multiple rooms and perhaps multiple floors, the difference in solar radiation intensity on the roof and the various walls would be much more important, and differences in convective heat transfer by surface would also become more important. The thermal comfort conditions inside the house will often vary from room to room, so thermostatic control will depend on

thermostat placement and internal heat and moisture flows. In a house with multiple zones, their thermostatic controls will be operating in parallel, requiring the economizer control algorithm to be redefined in a more complicated fashion.

A multi-room environment may present additional opportunities for free cooling under sufficiently advanced control. For example, it may be safe to overcool an east-facing non-sleeping room overnight to a temperature below the thermal comfort range. The morning sun may warm the room back to the heating setpoint before it comes into use. Similarly, if we overcool an area adjacent to an east-facing room, it may serve as a thermal reservoir to keep the east-facing room at a lower temperature as it receives morning solar radiation. These approaches would require thermostat algorithms with wider overnight setpoint ranges, as well as any forecasting considerations such as how sunny the morning is expected to be.

For all of these generalizations of the building design, however, it would seem impractical to continue the current analytic approach. Maintaining a lumped-capacitance nodal model for multiple interior spaces and dividing walls would quickly become a large and inflexible endeavor. To investigate how forecast-based economizer controls apply to more complicated building designs, it is recommended to develop the simulation of these controls within an established building simulation program. This requires significant effort and program expertise, but would offer improved accuracy and confidence of results as well as flexibility in selecting realistic building cases.

Tightening other simplifying assumptions would similarly motivate the change to an established and more realistic building simulation program. In particular, thermal bridging by structural elements, two-dimensional transport in walls, and corner effects are beyond what could be handled with reasonable effort in the current nodal model. Some of these, like thermal bridging, might be similar to a decrease in overall thermal resistance, which might have a relatively predictable effect against the benefits of the economizer, but overall, the effects on economizer performance seem unpredictable.

### 5.2.3 Wind and Infiltration Effects

The assumption of a fixed infiltration rate of 0.5 ACH is significant with regard to both magnitude and variation. In reality, infiltration rates vary widely over time and over different surfaces of a building. The airflow rate through a given crack or air path is driven by the difference in air pressure on either side, which depends strongly on wind speed and direction. Pressure is higher on the windward side of the house, pushing air in, and lower on the leeward side, letting air escape. Stronger winds tend to increase the pressure differences, the inflow and outflow rates, and thus the overall infiltration rate. This wind effect also complicates the rate of outdoor air exchange in multi-room houses.

A higher infiltration rate should tend to reduce economizer benefits. It speeds up the response of the indoor air to outdoor conditions, which is like reducing the thermal and moisture mass. Further, the infiltration replaces economizer airflow that might otherwise have been desired.

Higher wind speeds may also reduce economizer benefits through higher convection coefficients. The increased convective heat transfer will increase cooling load at times when the ambient air is warm and not useful for free cooling and decrease cooling load at times when the ambient air is cool and would offer free cooling. However, the delay imposed by thermal mass between convective transfer at the outer surface and when it reaches the indoor air makes this conclusion less certain and a potential subject for study.

Wind conditions will also have a large effect on air exchange rates through open windows. This would be an important factor to include in any simulation studies of control methods for free cooling by natural ventilation (e.g., automatic control of window opening and closing) rather than forced ventilation through an economizer.

### 5.2.4 Other Loads

This study has assumed a fixed internal sensible load of 200 W and the absence of any windows. More realistic cases may have sensible loads from occupants and electrical appliances at higher and widely variable levels and windows that allow considerable sensible solar heat gain. In general, the daytime solar gain should make the forecast-

based economizer control look better relative to the instantaneous economizer, by emphasizing the value of precooling for cool sunny days but not cool cloudy days. In other words, considering solar gain through windows enhances the variability of the overall cooling load and should make forecasting more valuable. Greater variability in the internal sensible load should have a similar effect.

We have also assumed the absence of an interior latent load, but in fact the occupants' respiration and water usage may contribute moisture to the indoor airspace. This leaves less of a margin for introducing outdoor air and still staying within the thermal comfort condition on relative humidity, so it should be expected to reduce economizer applicability. Whether it might make the forecast-based control more effective relative to the instantaneous control seems less clear.

### 5.2.5 System Costs

Although this study has been intended simply to study the potential of a forecast-based economizer approach with regard to building cooling load, we must eventually consider the costs of implementing the system against the savings it would offer. To install the economizer airflow components (ducting, inlets and outlets, and fan) can perhaps be priced in the low hundreds of dollars. For the electricity operation cost, we apply the estimated fan power load equation from Parker et al. (1987). If the economizer fan pressure difference is modest, on the order of 50 Pa, the power at 10 ACH is 80 W. Taking the Austin heavyweight case for example, the annual total economizer consumption would be about 40 kWh. At a typical residential air conditioning efficiency, the reduced building cooling load would save on the order of 70 kWh of air conditioning electricity consumption. Hence the fan power takes up more than half of the savings, which makes the case considerably more difficult.

The cost of the control system would be small in actual electronic components, but potentially large with regard to data acquisition, forecasting, and modeling. Accurate measurement of humidity (indoor and outdoor) remains challenging and somewhat expensive, and the relevant climatic conditions also include sky cover and wind. It might

be more efficient to make centralized climatic measurements (neighborhood or regional; current and forecast) and distribute them, but the system still has to measure the interior conditions of the building. Finally, the most difficult task is to create a building energy model that accurately predicts how a particular economizer airflow (i.e., damper position) and climatic condition will affect the evolution of the temperature and moisture conditions of the building airspace and envelope. Creating accurate simulation models for this purpose remains a matter of lengthy expert labor, even insofar as it can be done at all, at a cost possibly in the thousands of dollars. Almost all of this cost is specific to the benefits of forecast-based economizer control relative to instantaneous, which have not yet been proven to be significant. The economic case therefore appears overwhelmingly negative at present.

## 5.3 Other Economizer Impacts

One conceivable benefit of reducing cooling load would be to reduce peak energy demand, which would reduce the required air conditioning capacity and its initial equipment cost. However, the hourly pattern in cooling loads works against this opportunity. Free cooling and the thermal storage effect of overnight precooling replace air conditioning load in the early part of the day, but as the day progresses the indoor air and thermal mass typically reach the cooling setpoint temperature and the air conditioning system is needed. Then in the afternoon, when the peak cooling loads generally occur, the air conditioning load is unaffected by the free cooling that was used in the morning. Unless the thermal mass is large enough to provide stored cooling into the afternoon of peak-load days, the design load of the air conditioning system is unaffected. For example, in the heavy-construction home studied here, the design load, as determined by the $98^{th}$ percentile of hourly cooling loads, is reduced only 1% with the forecast-based economizer compared to without an economizer.

A related factor works against the economizer system in reducing electrical consumption. The energy efficiency ratio (EER), giving watts of sensible cooling per watt of air conditioning electrical load, decreases as the temperature increases in the heat

sink outside the condenser of a vapor compression cycle. In a typical residential system, this heat sink is the outdoor air, which is generally warmest in the afternoon. Therefore, the cooling load replaced by free cooling in the morning had been at a higher EER, and the remaining cooling load in the afternoon is typically at a lower EER. This implies a lower average EER, reducing the impact of any savings in indoor cooling load. However, another system type like a ground-source heat pump should be unaffected by this issue, since the underground temperature is largely insensitive to time of day.

## 5.4 Algorithmic Alternatives

On our test cases so far, we have found only very weak benefits in reducing cooling load from applying a forecast-based economizer control algorithm. We can consider whether the algorithm can be improved to achieve better energy savings.

One approach would be to account for the limiting factor of humidity more formally in controlling the introduction of outdoor air. This might be based on enthalpy rather than temperature, or jointly with it, to evaluate whether outside air is worth introducing, as has been done for traditional economizer controls. When indoor humidity is well below the thermal comfort limit, temperature is still the relevant consideration. When near the humidity threshold, enthalpy would become more important.

Even more explicit for managing humidity would be to extend the forecast-based algorithm of section 4.3.1 to control the economizer airflow rate $\gamma_{fcast}^{\tau}$ on both temperature and relative humidity directly. Currently the algorithm keeps a temperature $T_{min}$ below which the current indoor temperature should not be reduced without risking overcooling and increasing the heating load. $T_{min}$ is maintained iteratively as the forecast-based algorithm proceeds backwards through time. The extension would be to track also a partial vapor pressure $P_{max}$ from the backwards iteration, above which the indoor vapor pressure should not be increased by economizer airflow, so that upcoming moisture loads don't carry indoor humidity above the thermal comfort threshold. This approach would probably require iteration between the energy balance equations and

moisture balance equations, either directly or as part of a combined nonlinear system of energy and mass balance equations to be solved.

Yet another control method would be to let the economizer run simultaneously with the air conditioner, to balance free cooling against powered cooling with dehumidification. The economizer airflow could be considered either as a separate intake or as an intake being fed through the air conditioner and cooling coils before entering the room.

## 5.5 Conclusions

Based on some simple test cases and a simplified heat and moisture transfer model, the concept of a forecast-based economizer does not present clear and strong benefits in saving cooling energy or expanding the range of climates where economizers are valuable for residential application. Cooling loads can be reduced dramatically, but only at the cost of unreasonably elevated indoor humidity profiles. In effect, we have again illustrated the tradeoff between free cooling and indoor humidity control rather than overcoming it.

To investigate further, we could continue or extend somewhat the current analysis methodology with regard to wider ranges of climates, different ranges of thermal and moisture mass and internal and solar loads, and greater variation in wind conditions and infiltration rates. On the other hand, for more realistic building structures and internal layouts, we should write forecast-based economizer control modules for an existing and much more accurate building simulation program such as TRNSYS or EnergyPlus.

The conditions of the tests so far have been favorable to the forecast-based algorithm, due to the degree of foreknowledge of cooling loads. These loads will often be difficult to predict accurately. Therefore, the weak results so far argue against the effort of extending the analysis methodology either by balance equations or established software. It would be better to pursue improved economizer control algorithms as discussed in section 5.4, and if they have more favorable cooling load savings, then to refine the analytic methods and test cases.

# References


Berdahl, P. and M. Martin. 1984. "Characteristics of Infrared Sky Radiation in the United States." *Solar Energy* 33(3/4): 331-336.

Braun, J. E. 1990. "Reducing Energy Costs and Peak Electrical Demand through Optimal Control of Building Thermal Storage." *ASHRAE Transactions* 96(2): 876–888.

Braun, J. E., K. W Montgomery, and N. Chaturvedi. 2001. "Evaluating the Performance of Building Thermal Mass Control Strategies." *HVAC&R Research* 7(4): 403–428.

Henderson, H. I. and K. Rengarajan. 1996. "A Model to Predict the Latent Capacity of Air Conditioners and Heat Pumps at Part-Load Conditions with Constant Fan Operation." *ASHRAE Transactions* 102(1): 266-274.

Henderson, H. I., D. B. Shirey, and R. A. Ranstad. 2003. "Understanding the Dehumidification Performance of Air-Conditioning Equipment at Part-Load conditions." CIBSE/ASHRAE Conference, Edinburgh, Scotland. Available at: http://www.cdhenergy.com/presentations/CIBSE-ASHRAE%20Scotland%202003%20Part-Load%20Dehumidification.pdf.

Hirsch & Associates. 2009. *eQuest*. Available at: http://www.doe2.com/equest/.

Incropera, F. P., D.P. DeWitt, T.L. Bergman, and A.S. Lavine. 2007. *Fundamentals of Heat and Mass Transfer*. 6th ed. Hoboken NJ: John Wiley.

Judkoff, R. and J. Neymark. 1995. *International Energy Agency Building Energy Simulation Test (BESTEST) and Diagnostic Method*. National Renewable Energy Lab. Available at: http://www.osti.gov/energycitations/servlets/purl/90674-GSjdmY/webviewable/.

Ke, Y. P. and S. A. Mumma. 1999. "Variable Air Volume Ventilation Control Strategies Analysed in Six Climate Zones." *International Journal of Energy Research* 23(5): 371–387.

Lo, L.J. 2005. "Integrated Device Control for Residential HVAC Load Reduction." Master's Thesis, University of Texas.

Marion, W. and K. Urban. 1995. *User's Manual for TMY2s: Typical Meteorological Years*. National Renewable Energy Lab. Available at: http://rredc.nrel.gov/solar/old_data/nsrdb/tmy2/.

Morris, F. B., J. E. Braun, and S. J. Treado. 1994. "Experimental and Simulated Performance of Optimal Control of Building Thermal Storage." *ASHRAE Transactions* 100(1): 402–414.

Parker, D. S., J.R. Sherwin, R.A. Raustad, and D.B. Shirey III. 1997. "Impact of evaporator coil airflow in residential air-conditioning systems." In Proceedings of the 1997 ASHRAE Annual Meeting, *ASHRAE Transactions* 103 Part 2: 395-405.

Parker, D. S. 2009. "Very Low Energy homes in the United States: Perspectives on Performance from Measured Data." *Energy and Buildings* 41(5): 512-520.

Pfeifer, Ulrich. 2006. *Math::Matrix*. CPAN public software repository. Available at: http://search.cpan.org/~ulpfr/Math-Matrix/Matrix.pm.

Rode, C. and K. Grau. 2008. "Moisture Buffering and its Consequence in Whole Building Hygrothermal Modeling." *Journal of Building Physics* 31(4): 333-360.

Spitler, J. D., D.C. Hittle, D.L. Johnson, and C.O. Pederson. 1987. "A Comparative Study of the Performance of Temperature-Based and Enthalpy-Based Economy Cycles." *ASHRAE Transactions* 93(2): 13–22.

Thermal Energy System Specialists. 2007. *TRNSYS*. Available at: http://www.tess-inc.com.

Tye, R. P. 1994. "Relevant Moisture Properties of Building Construction Materials." In *Moisture Control in Buildings,* ASTM Manual Series, ed. H. R Trechsel. Philadelphia: ASTM, p. 35-53.

U.S. Department of Energy. 2009. *EnergyPlus*. Available at: http://apps1.eere.energy.gov/buildings/energyplus/.

U.S. Department of Energy, Energy Information Administration. 2009 *Annual Energy Review*. Available at: http://www.eia.doe.gov/emeu/aer/contents.html.

York Products. 2008. *Technical Guide: Affinity R-410A Split-System Air Conditioners*. Available at: http://www.yorkupg.com/PDFFiles/350154-YTG-D-0509.pdf.

Zajac, B. 1998. *Math::Interpolate*. CPAN public software repository. Available at: http://search.cpan.org/~bzajac/Math-Interpolate-1.05/lib/Math/Interpolate.pm.

# Vita

David E. Kaufman holds a B.A. in Mathematics from Case Western Reserve University in Cleveland, OH, *summa cum laude*, Phi Beta Kappa, and an M.S. and Ph.D. in Industrial and Operations Engineering, specializing in Operations Research, from The University of Michigan, Ann Arbor. His Ph.D. dissertation was titled "Direction Choice in Random Walk Algorithms with Application to Global Optimization". He was an Assistant Professor of Industrial Engineering from 1993 to 1997 at The University of Massachusetts, Amherst, teaching graduate and undergraduate courses in optimization, stochastic processes. From 1997 to 2007 he was a technical staff member with AT&T Labs in New Jersey, undertaking a wide range of internal consulting projects in network capacity and reliability, software development, Voice over IP, and simulation modeling. He has published scientific papers in research journals including Operations Research, Journal of Global Optimization, and IEEE Transactions on Intelligent Transportation Systems, and he is co-author of two U.S. Patents. In January 2008, he entered the Graduate School at The University of Texas at Austin.

Permanent address: 4203 Canyonside Trail
Austin, TX 78731
david.e.kaufman@gmail.com

This thesis was typed by the author.